



Cite this: *Mater. Adv.*, 2024,  
5, 9175

Received 22nd July 2024,  
Accepted 8th October 2024

DOI: 10.1039/d4ma00739e

rsc.li/materials-advances

## Cyanuric chloride as a linker towards the synthesis of covalent triazine polymers: a review

Silpa Elizabeth Peter,<sup>a</sup> Paul Thomas,<sup>b</sup> P. Vairavel <sup>c</sup> and N. V. Anil Kumar <sup>a\*</sup>

Covalent triazine polymers represent a promising class of materials composed of aromatic electron deficient 1,3,5-triazine repeating units. They are synthesized from different triazine monomers, where cyanuric chloride is one such monomer. It is known for its high reactivity and easy availability and has garnered significant attention due to its nitrogen-rich, stable triazine rings, and hydrophilic nature. These versatile and flexible polymers are exploited due to their stable heteroatom-rich skeletons and porous nature. This review discusses an overview of the synthesis of various porous polymers based on cyanuric chloride, along with its applicability in different sectors, especially in environment protection and energy storage. It gives an insight into the current and future perspectives for developing such polymers.

## 1. Introduction

Researchers have been fascinated by porous materials for decades due to their versatility and efficiency in various applications. These materials include inorganic porous materials such as zeolites, clay,<sup>1</sup> and silica, as well as organic porous materials like activated carbon (AC) and metal–organic frameworks (MOFs).<sup>2–5</sup> Zeolites are hydrated forms of sodium aluminosilicates with small pore diameters,<sup>6</sup> while AC is carbon-rich material processed from non-renewable energy sources, limiting its further applications.<sup>7,8</sup> MOFs are composed of organic linkers coordinating with metal ions but suffer from chemical instability due to weak coordination.<sup>9</sup> Despite possessing good surface area and ordered porosity, these conventional materials lack stability and regeneration ability, which limits their further applications.<sup>4</sup>

Porous organic polymers (POPs) have recently emerged as a new generation of advanced materials.<sup>5</sup> Composed of organic linkers of lighter elements connected through covalent linkages, they possess stability towards temperature and adverse chemical environments.<sup>10</sup> POPs exhibit structural regularity with discrete pores, resulting in a large surface area.<sup>11</sup> Different synthetic protocols can be designed depending on the symmetry of linkers and functional groups, resulting in multi-dimensional networked structures of various geometry.<sup>12</sup> One of their remarkable advantages over traditional materials is their highly tunable structures, allowing them to be tailor-made for specific applications. Functional modification, such as

sulfonation, can be made possible even after synthesis. Once they polymerize, they stack on each other through different interactions.<sup>12</sup>

Covalent triazine polymers (CTPs) belong to the family of POPs and have attracted scientific interest due to their exceptional stability.<sup>5</sup> They are incorporated with aromatic 1,3,5-triazine systems (Fig. 1), rich in basic nitrogen atoms,<sup>13</sup> stable C=N bond, high surface area, ordered porosity, and tolerance to humidity.<sup>14</sup> CTPs are insoluble in most used solvents and can resist temperature changes to some extent. Due to the abundance of basic nitrogen,<sup>15</sup> different interactions are possible with metals, pollutants, and gaseous carbon dioxide, making them an alternative and regenerative polymer<sup>14</sup> in various applications, such as catalysts,<sup>14,16</sup> adsorbents,<sup>5,17</sup> electrodes, and sensors. Conjugating with aromatic systems enhances CTPs' stability,<sup>2</sup> and delocalization results in unique optical characteristics. Linking with electron-rich monomers can form donor–acceptor complexes, improving electronic properties.<sup>18</sup> The incorporation of triazine groups into these CTPs

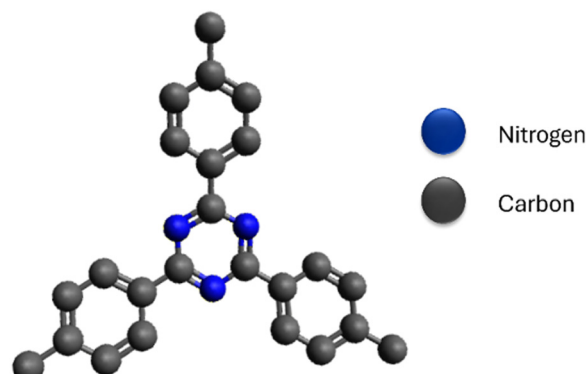


Fig. 1 Representation of repeating unit in CTP.

<sup>a</sup> Department of Chemistry, Manipal Institute of Technology, Manipal Academy of Higher Education, Manipal – 576104, India. E-mail: [mv.anil@manipal.edu](mailto:mv.anil@manipal.edu)

<sup>b</sup> Department of Physics and Technology, University of Bergen, Bergen, Norway

<sup>c</sup> Department of Chemical Engineering, Manipal Institute of Technology, Manipal Academy of Higher Education, Manipal – 576104, India

has resulted in altered surface properties. However, these modified polymers demonstrate enhanced performance when compared to similar polymers with benzene-rich structures.<sup>19</sup>

In 2008, Kuhn and his colleagues achieved a major breakthrough by creating the first triazine polymer through a complex trimerization of aromatic nitrile (benzene-1,4-dicyanonitrile). This process required high temperatures with sealed tubes, which posed challenges in terms of the potential decomposition of monomers.<sup>20</sup> Another research group, led by Cooper *et al.*, later developed CTPs at room temperature utilizing inert solvents.<sup>21</sup> However, both approaches had limitations in terms of the monomers that could be used due to decomposition or solubility issues. The preferred monomers were costly and required intricate synthetic pathways. Subsequently, researchers have managed to synthesize various triazine polymers (CTPs) using different monomers and customized synthetic conditions.<sup>22</sup> However, developing a simple and scalable method for creating these CTPs has proven to be quite interesting.

2,4,6-Trichloro-1,3,5-triazine, also known as cyanuric chloride, is a fascinating compound that is gaining attention as a monomer for CTPs (Fig. 2). These compounds are characterized by their heterocyclic, planar,<sup>22</sup> symmetric ( $D_{3h}$  point group), and rigid molecular structure,<sup>5</sup> with the chemical formula  $C_3N_3Cl_3$ .<sup>23</sup> This crystalline white solid is synthesized through the trimerization of cyanogen chloride at high temperatures and has a distinct pungent odor. The molecular structure resembles that of aromatic benzene, with alternating carbon and nitrogen atoms and three chlorine substituted to carbon atoms.<sup>24</sup> Despite their rigidity, these compounds are readily available, exhibit low toxicity, and have found applications in the chemical industry as an alternative halogenating agent.<sup>24</sup> They are particularly useful for activating carboxylic acids and alcohols into their derivatives. They serve as important precursors in the synthesis of triazine intermediates in the production of pesticides (such as atrazine<sup>25</sup>) and dyes.<sup>26</sup> More recently, there has been interest in their application as cross-linking agents in polymers.<sup>24</sup> This is made possible by the presence of labile bulky chlorine atoms, which provide selectivity with different nucleophiles.<sup>27,28</sup> The incorporation of triazine rings contributes to the stability and enhanced properties of these compounds for various applications.<sup>23</sup>

Appreciating the specific role of cyanuric chloride in organic reactions, this review offers a comprehensive overview of various CTPs (cyanuric chloride-based polymers). Although considerable research has been performed on these polymers, there is a lack of comprehensive analysis of their diverse applications.

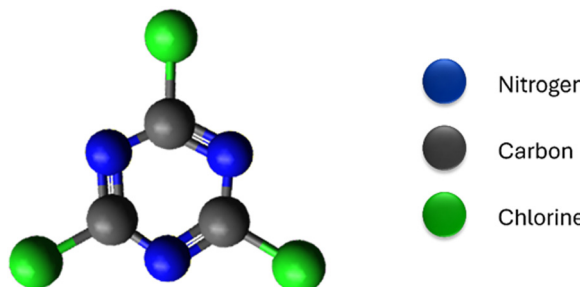


Fig. 2 Cyanuric chloride linker.

To the best of our knowledge, Jain *et al.*<sup>29</sup> and Sethiya *et al.*<sup>24</sup> have reviewed the role of cyanuric chloride as a catalyst in organic reactions. This review presents an extensive compilation of literature on different CTPs, including various synthetic protocols and their applications in the fields of energy, environment, and healthcare, providing a broad outlook.

## 2. Synthetic approaches

Let's explore the synthetic approaches that utilize cyanuric chloride as a linker for forming porous polymers.

### 2.1. Nucleophilic substitution polymerization

Nucleophilic polymerization is a reaction where an electron-rich nucleophile substitutes the functional group of an electron-deficient system. In this process, cyanuric chloride acts as an electron-deficient electrophile, and typically, the chlorine atoms are replaced by the protons of  $C_2$  or  $C_3$  symmetric amines or alcohols.<sup>17,30</sup> The nucleophile, amine attacks one of the chlorine atoms in the cyanuric chloride, forming a tetrahedral intermediate. Base abstracts the proton from the amine, restoring aromaticity by leaving negatively charged chloride ions to depart. Chloride ions combine with proton eliminates as  $HCl$  and thereby regenerating the base. Similarly, the other two chlorine atoms undergo nucleophilic substitution directing the polymerization (Fig. 4). The significance of this method lies in the concept of metal-free polymerization in mild, inexpensive conditions.

In 2019, Yadav *et al.*<sup>31</sup> synthesized a CTP-01 by nucleophilic substitution of *p*-amino phenol ( $C_2$  amino alcohol) in the presence of potassium carbonate as a base (Fig. 3). It is used as an effective catalyst for amide synthesis. Over the years, different combinations of amines/alcohols with cyanuric chloride (Fig. 4) have resulted in countless polymers of synthetic feasibility and applications.

Mostly, methods of synthesizing POPs require using costly solvents that need high temperature and pressure conditions and toxic catalysts.<sup>32,33</sup> Additionally, some of the building blocks are insoluble in the solvent medium, which can reduce the effectiveness of the reaction. As a result, more environment-friendly approaches can be utilized, such as the solvent-free solid-state method.<sup>34</sup> In 2017, Verma *et al.* developed a CTP from cyanuric chloride and urea using a solid-state approach by heating at 140 °C. Even though the surface area was too low, it behaved as an efficient catalyst for sequestering carbon dioxide due to its basic nature.<sup>35</sup>

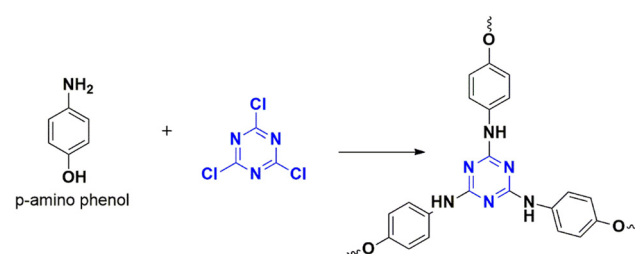


Fig. 3 Scheme for the synthesis of CTP-01.



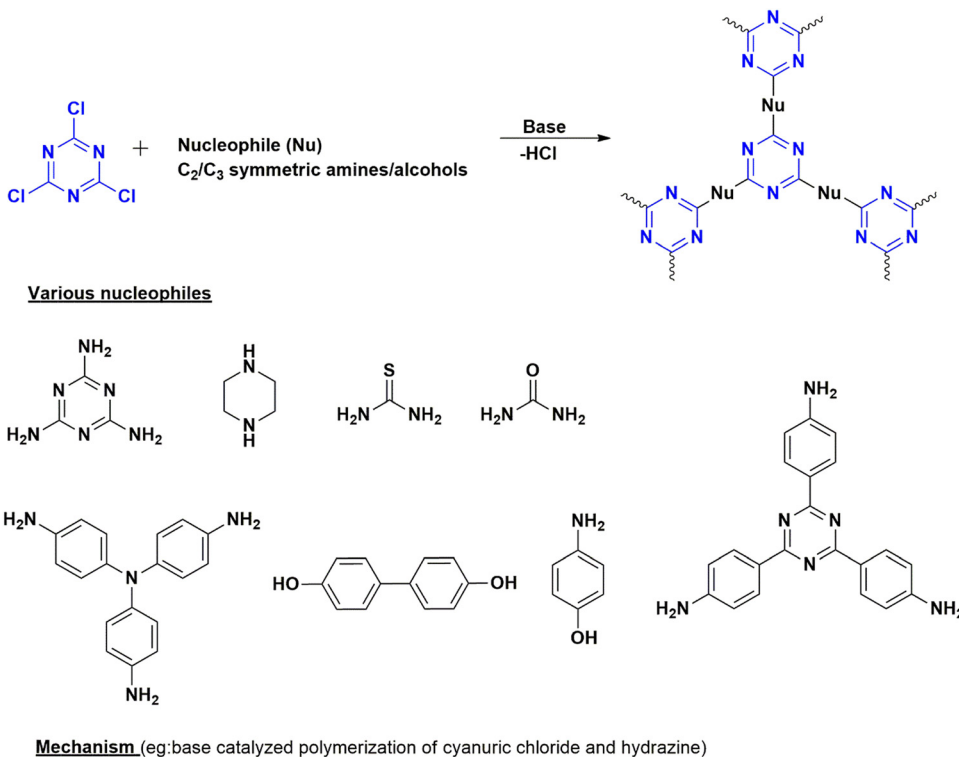


Fig. 4 Scheme for the synthesis of CTP by nucleophilic substitution reaction with different monomers along with the mechanism.

## 2.2. Friedel-Crafts reactions

These are C–C bond-forming electrophilic reactions in aromatic systems involving an alkyl halide and arenes in the presence of a Lewis acid (methyl sulfonic acid<sup>36</sup> or  $\text{AlCl}_3$ ) in inert solvents – the reaction proceeds by the attack of electron-deficient cyanuric chloride on an electron-rich monomer. Lewis acid, anh.  $\text{AlCl}_3$  reacts with cyanuric chloride, forming a carbocation (Fig. 6(b)). This electrophilic carbocation further reacts with electron-rich arenes, forming a cyclohexadienyl cationic system losing its aromaticity. The aromaticity is restored by deprotonation ultimately forming a new C–C bond.<sup>37</sup>

The preferred catalysts are either methanesulfonic acid or anhydrous aluminum chloride. The choice of catalyst depends upon the reactivity of the building blocks.<sup>38</sup> Methanesulfonic acid is a non-toxic liquid catalyst with high thermal stability and is soluble in all ratios of monomers.<sup>39</sup> It can improve the efficiency of the reaction, favoring *para*-position-oriented reactions<sup>38,40</sup> and making it suitable for commercial applications. One of the advantages is the environmentally friendly

byproducts formed during the polymerization,<sup>41</sup> along with the ease of separation using water.<sup>40</sup> Anhydrous aluminum chloride is a solid catalyst, which can limit the solubility of linkers<sup>39</sup> and intermediate fragments to a certain extent and promote the undesired interaction of precursors during polymerization.<sup>38</sup>

Putthiaraj *et al.* (2016) synthesized a polymer from cyanuric chloride using different linkers, such as triphenylethylene and tetraphenyl silane, for carbon dioxide adsorption,<sup>42</sup> followed by Stella *et al.* (2019 and 2020) designed a polymer from triphenyl benzene<sup>43</sup> and biphenyl<sup>44</sup> for supercapacitor applications. All these polymerizations were catalyzed by anh.  $\text{AlCl}_3$ .

Methanesulfonic acid was used to catalyze the reaction of cyanuric chloride with sandwiched structured ferrocene<sup>39</sup> by Fu *et al.* (2015), which was later doped with iron atoms for its applications in gas storage. Similarly, a series of polymers for capturing iodine and detecting 2,4-dinitrophenol were reported in this approach by Geng *et al.* (2017 and 2018) from tetraphenyl derivatives of phenylene diamine, melamine,<sup>36</sup> and biphenyl<sup>40</sup> and by Fang *et al.* (2022) from 3,4-ethylenedioxythiophene and 2,2'-bithiophene.<sup>45</sup>

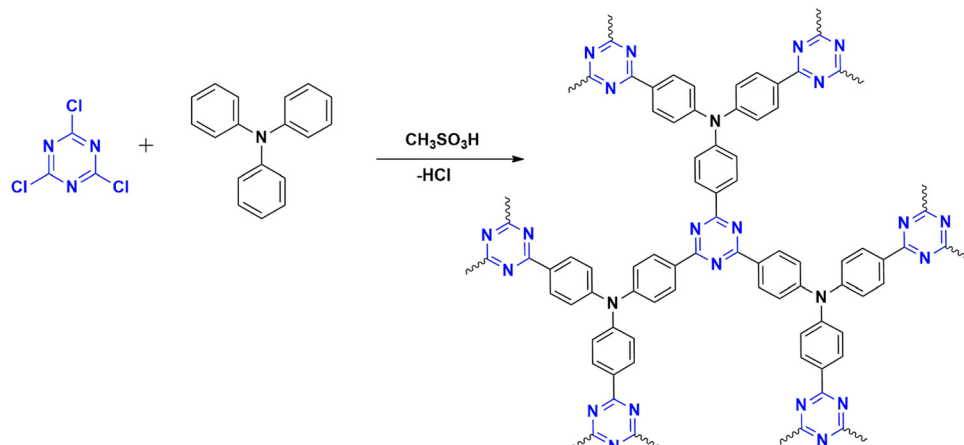


Fig. 5 Scheme for synthesis of CTP-02.

Xiong *et al.* (2014) developed a polymer using triphenyl methane (CTP-02; Fig. 5) and tetraphenyl silane with a high yield in methane sulfonic acid, but the reaction with benzene and biphenyl using  $\text{AlCl}_3$  resulted in a low yield.<sup>41</sup> Similarly, Geng *et al.* (2020) compared the efficiency of both catalysts using a tetraphenyl derivative of phenylene diamine polymerized with cyanuric chloride. This protocol had a high yield in methane sulfonic acid but a low yield in  $\text{AlCl}_3$ .<sup>38</sup>

Until now, many polymers (Fig. 6(a)) with high yield and other significant properties have been developed based on this protocol<sup>43,44</sup> attributed by the wide applicability, low cost, and flexibility of the reaction conditions. The drawback of this protocol is the irreversible nature of polymerization, resulting in the production of amorphous polymers with side products that affect its large-scale production.

As an alternative to this approach, Troschke reported reactions using the mechanochemical milling technique as a green strategy, which reduces the usage of toxic solvents and can scale up the reaction.<sup>46</sup> The density of the milling ball defines the reaction's progress as it imparts energy. As a reference, they developed a porous polymer from cyanuric chloride and carbazole using tungsten carbide as the milling ball, with a 90% yield achieved in one hour. In comparison to conventional CTPs (sealed ampule synthesis), these CTPs (mechanical) had a high C/N ratio without any carbonization. Monomers with extensive conjugation can be utilized in this reaction with high yield. Even unreactive monomers, such as benzene, reacted with low yields. The solubility of monomers in a particular solvent is a decisive factor and challenging for synthesizing polymers; therefore, this green method can be used for such monomers with high yields. The abrasions due to the milling ball affect the purity of the polymer, which must be improvised.

Cyanuric chloride itself is rich in triazine core; there is no need for further functionalization, which substantially expands the range of probable monomers.<sup>47</sup>

### 2.3. Post-functional modification

In addition to these polymerizations, another significant advantage of these materials is post-functional modification, which enhances the efficiency of the polymer by incorporating different

functional groups based on its applications. Sulfonation, an electrophilic substitution, is a dominant reaction in organic chemistry where hydrogen atoms (aromatics) are replaced by the electrophile sulfur trioxide ( $\text{SO}_3$ ). It incorporates the hydrophilic character, making it suitable for use in aqueous mediums.<sup>48</sup>

Generally, incorporating these modifications improves the efficiency of polymers in different applications as these acidic functional groups can capture moisture/water and can release protons for proton-conducting membranes.<sup>49</sup> It improves the interaction with different pollutants in the water, making it a superior adsorbent. Additionally, it can catalyze several organic reactions due to its better reactivity.<sup>50</sup> For example, Raza *et al.* developed an aromatic porous polymer by a cascade reaction initiated by Friedel-Craft alkylation of cyanuric chloride, triphenyl benzene and trimesoyl chloride,<sup>51</sup> followed by sulfonation with acidic  $\text{SO}_3\text{H}$  and later Schiff base condensation with ethylene diamine and incorporated with Pd metal. It was explored as an efficient catalyst for multicomponent reactions. The same group explored the sulfonation of triazine polymer CTP-03 from cyanuric chloride and *p*-terphenyl (Fig. 7) with palladium incorporated for hydrogenation esterification of nitrobenzoic acid.  $\text{SO}_3\text{H}$  acts as a site for esterification.<sup>52</sup> Babaie *et al.* reported a sulfonated (1,4-butane sulfone) porous polymer (cyanuric chloride and melamine) on mesoporous silica as a catalyst for synthesis of hydroxymethylfurfural from fructose.<sup>22</sup> Taheri *et al.* prepared a polymer from cyanuric chloride and triphenylmethane,<sup>53</sup> followed by modifications with  $\text{SO}_3\text{H}$  for adsorption of basic blue 41 and basic blue 46. Although this functionalization affects the surface properties (by blocking the pores), it improves the efficacy of the system for different applications.<sup>48</sup>

## 3. Structure–property relationship of CTPs

The structure of CTPs is reinforced by robust alternating  $\text{C}=\text{N}$ ,  $\text{C}-\text{N}$  linked stable triazine rings. These linkages are formed by irreversible polymerization, imparting chemical and thermal stability to the polymers, even in harsh conditions.<sup>54</sup> Due to their nitrogen-rich nature,<sup>55</sup> CTPs can



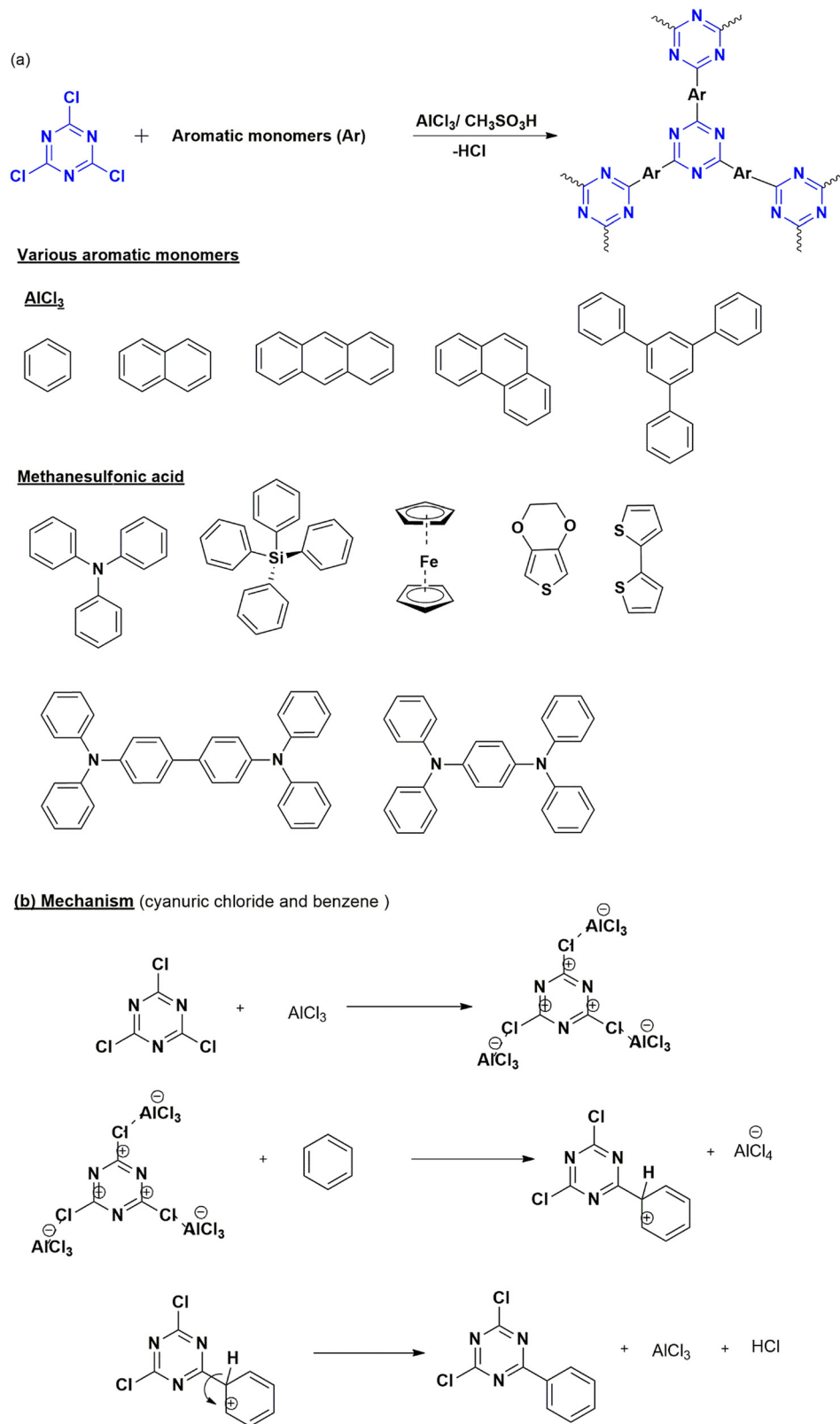


Fig. 6 (a) Scheme for the synthesis of CTP by Friedel-Crafts reaction with different monomers along with the (b) mechanism.

effectively capture different molecules, such as pollutants and gases, making them versatile for various applications. When these triazine rings are polymerized with different aromatic or

electron-rich moieties, the energy of the system is reduced through effective conjugation, thereby enhancing their stability.<sup>23</sup>

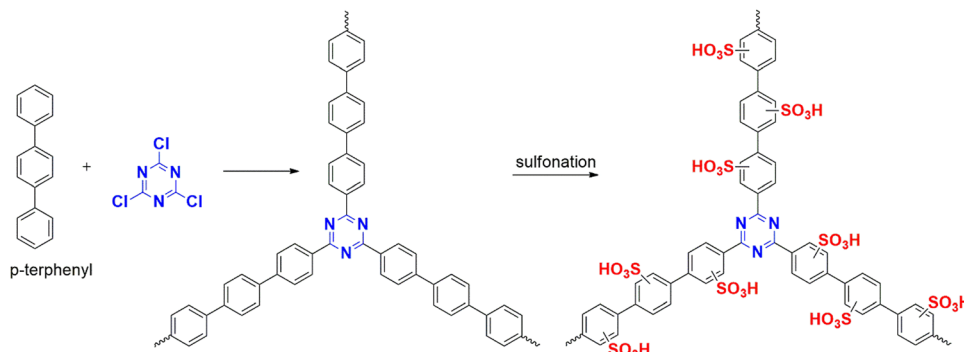


Fig. 7 Scheme for synthesis of CTP-03 followed by sulfonation.

The pore structure of CTPs can be tailored depending on the symmetry and length of the connecting linkers, allowing hexagonal, trigonal, or tetragonal pore structures.<sup>55</sup> Furthermore, modifications can be made to these polymers, providing an added advantage. The chemical nature of the linkers renders the polymer with acidic/basic (charged) and hydrophilicity. As light-weight materials, CTPs find applications in various fields.<sup>56</sup>

CTPs exhibit structural regularity and defined pores due to their covalent linkages, and they are typically amorphous or semicrystalline in nature as a result of irreversible polymerization.<sup>23</sup> These polymers possess characteristic surface area and porous properties, making them suitable for gas adsorption, catalysis, and pollutant removal.

In the past, organic reactions were predominantly carried out using homogeneous catalysts,<sup>57,58</sup> which often involved expensive solvents and led to low efficiency due to purification requirements.<sup>31</sup> However, CTPs are insoluble in water and most common solvents, providing chemical stability. Consequently, these polymers are widely utilized in catalytic applications owing to their heterogeneous nature,<sup>59</sup> which allows for easier separation. They can also serve as solid support to immobilize nanoparticles and enhance their effectiveness in various catalytic processes.<sup>60</sup> Additionally, the stacked polymeric layers act as channels for charge transport, making them effective as photocatalysts.<sup>61</sup>

The porous properties of CTPs are significantly influenced by the synthesis conditions, including temperature, pressure, solvent type, and catalyst used. These structure–property relationships are crucial in determining the suitability of CTPs for various applications.

## 4. Applications

As introduced in this paper, CTPs possess specific remarkable properties, such as porosity with a large surface area, thermal and chemical stability, inexpensive linkers and nodes, and the ability for post-modification. These properties make CTP an excellent candidate for various applications such as catalysis, adsorption, sensing, drug delivery, and energy storage devices (Fig. 8). This is possible due to the stable, flexible, and heteroatom-rich triazine systems. The following sections summarize all these applications.

### 4.1. Heterogeneous catalyst

Catalysts are substances that speed up the reaction by lowering the activation barrier without being used up.<sup>15</sup> They are pivotal in most transformations that make up this chemical world, including human beings. Enzymes or metal-based molecules have initially dominated the field of catalysis. The homogeneous nature of these catalysts makes them challenging to remove, leading the researchers to explore the development of efficient heterogeneous catalysts. This pursuit is motivated by the need to minimize the use of expensive and toxic reagents, which currently pose significant challenges to the field. Recently, porous polymers and nanoparticle-encapsulated polymers have occupied the field of catalysis, being insoluble and inert in harsh conditions.

**4.1.1. Organic transformations.** The CTPs (cyanuric chloride with different linkers) as a catalyst towards different organic transformations, along with their surface properties, are listed in Table 1.

**4.1.1.1. Multicomponent reactions.** Mizoroki–Heck coupling is an inevitable protocol for forming C–C bonds, which

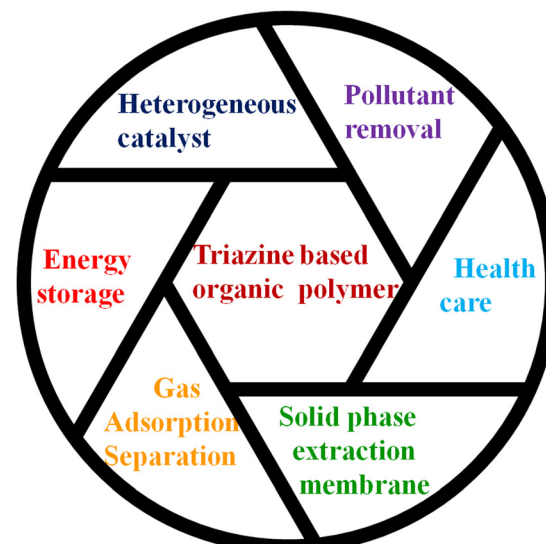


Fig. 8 Applications of CTPs.



Table 1 List of CTPs (cyanuric chloride with different linkers) as a catalyst towards different organic transformations, along with their surface properties

S. No.	CTP	Different linkers	Catalytic reaction	Surface area ( $\text{m}^2 \text{ g}^{-1}$ )	Ref.
1	CTP-04	Dihydroxy biphenyl	Mizoroki–Heck coupling reaction	146	60
2	CTP-05	Tetraphenyl amine porphyrin	Oxidation of aryl alkanes	621	62
3	CTP-13	Phenylene diamine	Epoxidation of carbon dioxide	35.4	63
4	CTP-12	2,4,6-Trihydrazinyl 1,3,5-triazine	Epoxidation of carbon dioxide	51.2	64
5	CTP-06	Melamine	Knoevenagel reaction	850	15
6	CTP-06	Melamine	5-Hydroxymethyl furfural synthesis from fructose	157	22
7	CTP-01	<i>p</i> -Aminophenol	Synthesis of amide	248	31
8	CTP-07	Thiourea	Hydrogenation of nitroaromatics	90.2	16
9	CTP-11	Piperazine	Methanolysis of ammonia borane	369	65
10	CTP-06	Melamine	Conversion of phenylboronic acid to phenol	—	13
11	CTP-08	2,4,6 Tris( <i>p</i> -aminophenyl)triazine	Quinazoline synthesis	26.7	14
12	CTP-09	Guanidinium hydrochloride	C–Se coupling reaction	81.04	66
13	CTP-10	2,4,6 Triaminopyrimidine	Synthesis of benzimidazole	58.12	67

includes the foundation for many active ingredients in the medicinal world.<sup>68</sup> It is the coupling of alkenes and alkyl halide catalyzed by Palladium metal. Nanosized palladium suffers from aggregation and can leach out, blocking the catalytic sites. So, these particles need to be supported to enhance the catalysis. In 2014, Puthiaraj *et al.* developed a mesoporous polymer CTP-04 (Fig. 9) from cyanuric chloride and dihydroxy biphenyl, which has the dual function of supporting the metal and enhancing the catalysis.<sup>60</sup> The presence of heteroatoms like O and N binds with metal species, providing solid support for palladium particles. The as-made polymer was composed of cauliflower-shaped particles with partial crystallinity and a desirable BET surface area ( $146 \text{ m}^2 \text{ g}^{-1}$ ) and pore size of 2.34 nm. The reaction conditions were optimized using styrene and bromobenzene as model reactants with 30 mg of catalyst in a DMSO–water mixture for 10 hours in the presence of a 1 mmol potassium carbonate base at 90 °C. Alkyl bromides with electron-deactivating groups readily couple with alkenes with alkyl or alkoxy groups. Sterically hindered molecules undergo coupling with a long reaction time. Selectivity of bromide over chloride groups was observed. Pd-embedded porous polymer serves as an efficient catalyst with eight cycles of recyclability.

Metalloporphyrin is an enzyme containing metal ions that can catalyze different chemical reactions, mainly oxidation in drug metabolism.<sup>69</sup> Extensive research is conducted to fix this catalyst to a solid support, making them heterogeneous since the porphyrins are unstable. In 2015, Zou and his co-workers developed a porphyrinic framework CTP-05 (Fig. 10) from

cyanuric chloride and tetraphenyl amine porphyrin<sup>62</sup> with a uniformly porous structure of surface area of  $621 \text{ m}^2 \text{ g}^{-1}$ . The resulting CTP was finally metallated with manganese and compared with the analogous manganese metallated tetraphenyl porphyrin molecule. This heterogeneous catalyst could oxidize aryl alkanes in water under moderate conditions, including the oxidation of ethylbenzene to acetophenone with a yield greater than 99 percent. The porphyrinic metallic sites in CTP-05 are accessible for the adsorption of reactants and desorption of products due to their selective nature. The size of the substrate is inversely related to catalytic efficiency. They could recover the catalyst and retain its ability for 15 more cycles (Fig. 11). They compared CTP-05 with its homogenous counterpart, which could catalyze the ethylbenzene oxidation with a yield of 91 percent. It can be reused for three cycles, highlighting the exceptional stability of porous polymers. An unusual behavior in the case of 4-ethyl biphenyl is that the homogenous catalyst surpassed the heterogeneous catalyst.

The creation of carbon–carbon bonds has necessitated extensive research over the last years of chemical evolution, as they form the basis of the synthesis of products in everyday life.<sup>70</sup> Previously, the Knoevenagel reaction contributed to quite a few of these formations. It involves reacting carbonyl-rich compounds with active H compounds in basic conditions. Different homogeneous and metallic-based catalysts have been investigated; however, recent sustainability issues prompted the researchers to try out the green-friendly heterogeneous catalyst for the Knoevenagel reaction. Usually, amine-rich catalysts are utilized.<sup>71</sup> In 2018, Chaudhary *et al.* adopted microwave synthesis for the nanoporous polymer (CTP-06; Fig. 12) by condensing triazine-rich melamine and cyanuric chloride.<sup>15</sup> CTP shows amorphous nature, a BET surface area of  $850 \text{ m}^2 \text{ g}^{-1}$  with spherically arranged particles of micropores (1.3 nm) and mesopores (4.1–6.9 nm). They investigated the Knoevenagel reaction between the active compound malononitrile and different aryl aldehydes by optimizing various parameters for excellent yield. The reaction conditions were optimized to 5 mg of CTP-06 in dioxane–water solvent for half an hour with exceptional outcomes. Better solubility of reacting molecules and basicity (adsorption of  $\text{H}_2\text{O}$  to N-rich sites) enhances efficiency. Thus, CTP-06 can be a future effective catalyst (compared to the metal catalyst) with minor catalytic activity loss after eight cycles.

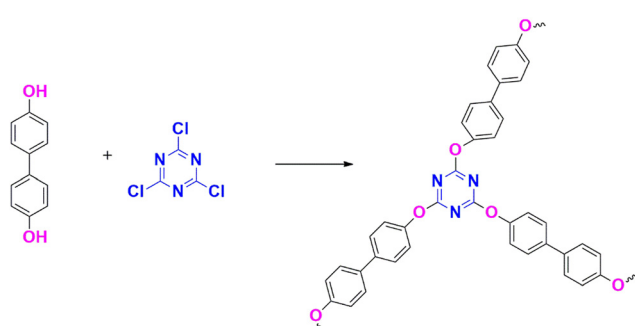


Fig. 9 Schematic formation of CTP-04.



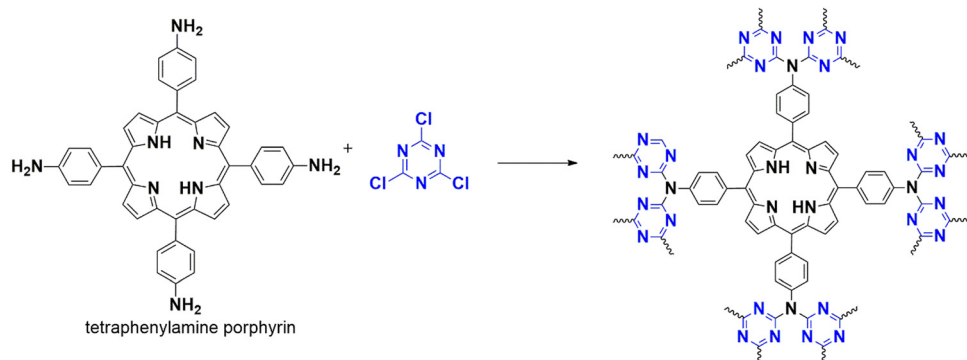


Fig. 10 Scheme for synthesis of CTP-05.

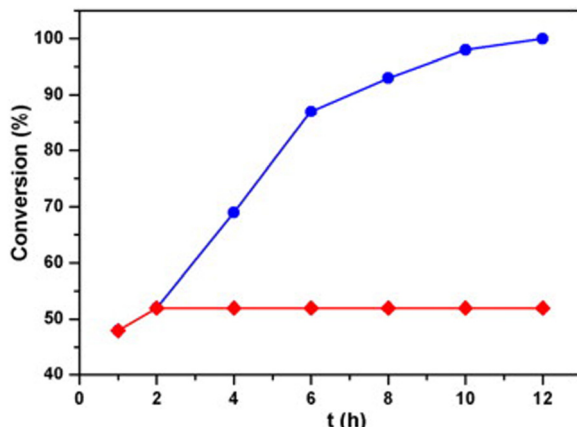


Fig. 11 The efficiency of catalytic conversion of ethylbenzene by CTP-05 over time (blue dots). The catalyst was separated by centrifugation after 2 h (red dots). Adapted from ref. 62 Copyright 2015 Elsevier.

The heteroatom functionality, amide group, is prevalent in most of the biologically relevant molecules<sup>72</sup> and other chemical products<sup>73</sup> used in our day-to-day life.<sup>74</sup> The reported protocols for amide synthesis demand extreme conditions and harmful chemicals. A direct combination of acid and amine-forming amide linkage needs to be inspected. Porous networked structures are efficient catalysts in many reactions, as they are insoluble in common solvents with excellent stability. An asymmetric porous polymer CTP-01 (Fig. 3) was developed by Yadav and his co-workers in 2019 as a powerful catalyst for the direct synthesis of amide mediated in moderate conditions with zero additives.<sup>31</sup> The CTP prepared by this method

possesses a high specific surface area and pore size ( $248 \text{ m}^2 \text{ g}^{-1}$ , 2.72 nm), good stability, and semi-crystallinity. Porous nature was confirmed from the morphology of irregular clustered particles with stacking. A wide range of substrates was considered for the activity, and it was observed that the nucleophilic nature of amines directs the reaction (favoring electron-donating groups). The reaction conditions are optimized to 10 mg of CTP-01 in dioxane solvent under room temperature. The selectivity of the catalyst was studied further and observed that in a mixture of aniline, benzoic acid, and phenol, the reaction favored the formation of amide over an ester. The catalyst selects acid rather than an ester compound in a mixture of methyl benzoate, aniline, and benzoic acid. The catalyst can be reused for nine cycles with agreeing results. Thus, CTP-01 can be a promising catalyst for many reactions with improved yields within a short duration.

The same group has developed a catalyst composed of a heterogenous N-rich polymer to hydrogenate nitroaromatics.<sup>16</sup> Nitro-derived compounds can harm living organisms, but their reduced amino derivatives are useful as starting materials for many valuable products. The polymer CTP-07 is synthesized from cyanuric chloride and thiourea through a solid-state approach (Fig. 13) and later uniformly confined with palladium nanoparticles (Pd@CTP-07). This approach prevents the agglomeration of metal particles while exposing them to catalysis sites. The obtained amorphous CTP exhibited very high thermal and chemical stabilities with irregular clustering of particles agreeing the porous nature. Besides, the specific surface areas of CTP reached  $90.2 \text{ m}^2 \text{ g}^{-1}$  with pore size of 1.9 nm. For example, when nitrophenol was used as the starting material, the polymer showed a better catalytic property with a high yield quickly, accompanied by a color change. Pd@CTP-07 and sodium borohydride were the preferred catalysts. It was observed that in the absence of these catalysts, no reaction occurred. The catalyst can be reused for nine cycles and can convert a wide range of reactants with high yield, regardless of their nature. The researchers also studied the effect of surfactants on nitro compounds, which are pollutants in water. They found that the polarity of these surfactants affected the catalytic performance, as denoted by the order: nitrogen > formic acid > ammonium hydroxide. Even the steric hindrance of the nitro

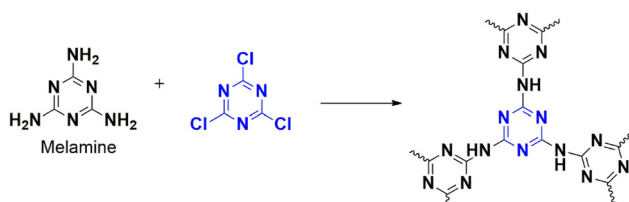


Fig. 12 Scheme for synthesis of CTP-06.



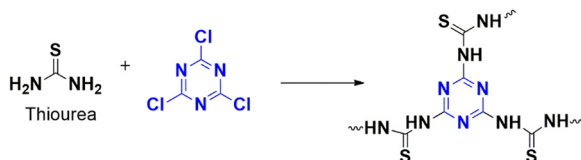


Fig. 13 Scheme for synthesis of CTP-07.

group affected the reaction rate, with 2,4,6 trinitro < 2,4-dinitro < nitrophenol.

Researchers worldwide are interested in environmentally friendly, green approaches for synthesizing intermediates, especially from biomass, due to the decline in natural resources. Babaei *et al.* developed a polymer that is supported on amino-modified mesoporous calcined silica (SBA-15) and acts as a heterogeneous catalyst for generating 5-hydroxymethylfurfural (HMF) from fructose, with a yield of 78%.<sup>22</sup> Catalysts are usually characterized by high surface area for the accessibility of reactants towards the active pockets. Here, the polymer, CTP-06 is synthesized from triazine derivatives, cyanuric chloride, and melamine (Fig. 12), then grafted on amino-functionalized SBA-15. It is later modified by sulfonating to improve its acidic nature, which helps in the dehydration of biomass. The resulting CTP possess mesoporous, amorphous nature and surface areas ( $11\text{ m}^2\text{ g}^{-1}$ ) with regular open channels (1.7 nm; sponge morphology). The reaction conditions were optimized for maximum yield. Different biomasses with varying yields were considered under optimized conditions, including fructose, glucose, sucrose, and maltose. Fructose yielded the highest, followed by sucrose, glucose, and maltose. For sucrose and maltose, conversion involved three levels: hydrolysis, isomerization to fructose, followed by dehydration. This might be a reason for the decrease in yield. Even though glucose yielded less, increasing the reaction time could be improved to 45%. The catalyst was reused four times with a comparable yield, where the reported catalytic reaction resulted in low yield with difficulties. CTP-06-SO<sub>3</sub>H/SB catalyst claims to be an alternative catalyst with high yield in short durations.

Phenol is an inevitable ingredient in the chemical industry as it produces various essential molecules, including those

used in medicine, fertilizers, dyes, and cosmetics. In a study, Sadhasivam *et al.* designed a polymer that incorporated copper nanoparticles as a catalyst to convert the phenyl derivative of boronic acid to phenol with over 96% yield in a short time using peroxide oxidation.<sup>13</sup> The polymer, CTP-06 was made from heteroatom-rich monomers, cyanuric chloride, and melamine (Fig. 12), later grafted with copper. These porous polymer exhibited a partial crystalline ordered smooth morphology. Phenyl boronic acid was used as the model system to study the efficiency of this polymer. The optimized reaction was performed at room temperature and yielded 99% within 10 minutes. The catalyst proved more efficient when electron donors rather than electron acceptors were used. The number of rings in the molecule also significantly affected the yield, with phenyl derivatives being the most efficient, followed by naphthyl and pyrene derivatives. However, when a pyridine derivative was used, the yield decreased due to the coordination of the metal nanoparticle with N-containing pyridine. Bulky substrates were observed to lower the yield of the reaction. The Cu-CTP-06 catalyst was reused five times with minimal difference in yield. Compared to other reported catalytic systems, this catalyst is an excellent option for oxidizing phenylboronic acid without external additives.

In 2020, Subodh *et al.* designed and developed an efficient triazine-based polymeric catalyst (CTP-08) by condensing triazine-abundant units (Fig. 14): cyanuric chloride and 2,4,6-tris(*p*-aminophenyl)triazine(TAPT).<sup>14</sup> The synthesized CTP has a hexagonal pore structure (2.86 nm) with a surface area (26.7 m<sup>2</sup> g<sup>-1</sup>). Being amorphous with irregular aggregation of particles are observed in morphological studies. This catalyst supports the synthesis of quinazolines and its derivatives. The quinazolines are nitrogen-rich cyclic compounds that can be associated with a variety of pharmacological activities.<sup>75</sup> Recent protocols for quinazoline synthesis are well known, but these protocols have some challenges, such as catalyst solubility and by-product formation. For the first time, a polymeric catalyst is utilized for the multi-component one-pot synthesis of quinazoline. The model reaction is between amino aryl ketone and aryl aldehydic system. After optimizing the conditions

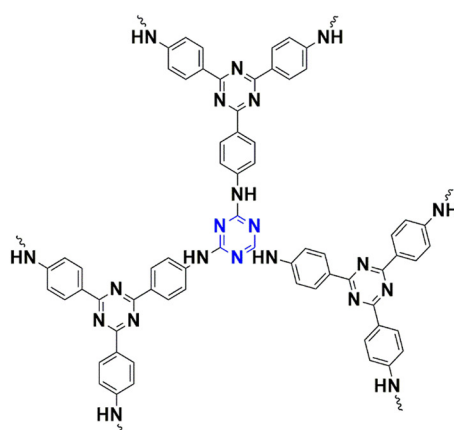
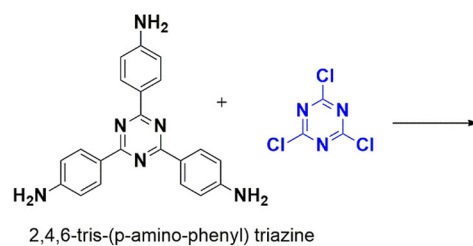


**Fig. 14** Scheme for synthesis of CTP-08

(ethanol solvent, 60 °C reflux), a wide range of aldehydic systems were considered. From the yields obtained, it was observed that electron-withdrawing groups favor the reaction more than electron donors. The active site responsible for catalytic activity in the polymer was determined by converting benzaldehyde using the catalyst CTP-08 and TAPT building block. TAPT, being a homogenous catalyst, transforms benzaldehyde to quinazoline along with by-products. CTP-08, being a heterogeneous catalyst, selectively forms quinazoline. This suggests that the -NH group drives the transformation. CTP-08 can be reused for six cycles with agreeing results, opening a door for the applicability of porous polymers in multicomponent reactions.

Selenium is essential in the formation of many biologically functioning molecules as well as intermediates in many reactions. As a result, the coupling of C-Se bonds is crucial for chemists and biologists.<sup>76</sup> Yadav *et al.* published a report in 2020 about a new polymer, CTP-09 synthesized (Fig. 15) from cyanuric chloride and guanidinium hydrochloride.<sup>66</sup> Later, nickel nanoparticles were added to this polymer to enhance its catalytic ability. Polymeric particles possessed a sponge structure with amorphous ordering and surface area ( $81.04 \text{ m}^2 \text{ g}^{-1}$ ) and pore dimensions of 1.67 nm. The polymer supports the nanoparticles and can help synthesize diaryl selenides from haloalkanes using inexpensive selenium powder in benign aqueous solvents in room conditions within a short duration. The conditions for the coupling reaction were optimized using the model reaction of iodobenzene with selenium. 10 mg of polymer catalyzes the reaction in the presence of potassium carbonate as the base at room conditions for 3 hours in aqueous DMSO conditions (1:1). The substrate scope was studied extensively, as aryl chlorides failed for the reaction. Aryl iodides give high yield organoselenides compared to aryl bromides. The yield of the reaction was independent of the reactants' nature, whether electron donating or withdrawing groups were present. The uniform confinement of nickel nanoparticles on the N-rich stable framework leads to the overall efficiency of this heterogeneous catalyst.

Benzimidazoles represent a critical starting point in the development of drugs with various biological activities. These nitrogen-rich aromatic compounds are often employed to create different functional materials. However, traditional methods of synthesizing benzimidazoles from aldehydes and 1,2-phenylenediamines have certain shortcomings. Aswathy *et al.* have overcome these difficulties by using a porous polymer as a catalyst.<sup>67</sup> This catalyst polymer unites reactants while activating the aldehyde by providing binding sites for hydrogen bonding. As a result,

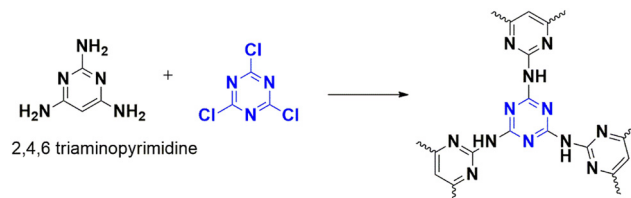


Fig. 16 Scheme for synthesis of CTP-10.

aryl-substituted benzimidazoles and their derivatives can be synthesized at room temperature. The catalyst, CTP-10 was synthesized from cyanuric chloride and triamine-derived pyrimidine (Fig. 16), resulting in a low surface area ( $58.12 \text{ m}^2 \text{ g}^{-1}$ ) due to the disorderly arrangement of layers (amorphous) with irregular pores (11.8 nm). Benzaldehyde and *o*-phenylenediamine were utilized as a model system to evaluate the efficacy of the catalyst, and its necessity was demonstrated by the fact that in its absence, the reaction proceeded without any yield but with the generation of unnecessary byproducts. In the presence of the catalyst, the yield improved due to the enhancement of basic nitrogen sites that promote the forward reaction. The substrate scope was also studied, and it was found that electron-deactivating groups yielded better results than electron-rich substituents. The catalyst can be reused for up to five cycles while retaining its activity. The reaction's mechanism was proposed and supported by computational approaches.

**4.1.1.2. Hydrogen generation.** Hydrogen is a promising energy source crucial for a sustainable and growing population. However, the challenge lies in the storage of hydrogen, which can be pretty tricky. Methanol reduction of ammonia borane is an attractive solution, as it can produce three equivalents of molecular hydrogen.

Recently, Li *et al.* developed a new framework, CTP-11 (Fig. 17) by combining cyanuric chloride and piperazine.<sup>65</sup> They then immobilized rhodium metal within the framework to create Rh/CTP-11. This approach helps prevent further leaching and agglomeration of the metal, reducing the catalytic efficiency. The polymer demonstrated a amorphous stacked structure with a superior surface area of  $369 \text{ m}^2 \text{ g}^{-1}$  (pores of 3.7 nm). Compared to metal nanoparticles, the framework is smaller and has exposed active sites for catalysis. However, pure framework CTP-11 was unable to catalyze the reaction. Only the rhodium-confined frameworks exhibited methanolysis at the highest rate compared to other reported catalysts. Additionally, Rh/CTP-11 can be reused up to five times, making it an environmentally friendly option. One of the significant advantages of this framework is its ability to

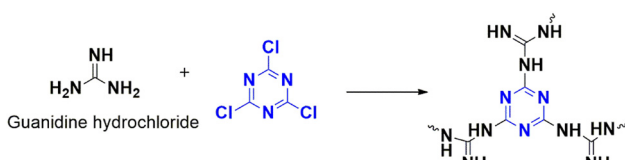


Fig. 15 Scheme for synthesis of CTP-09.

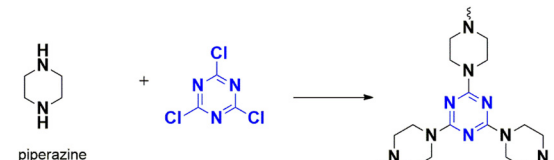


Fig. 17 Scheme for synthesis of CTP-11.



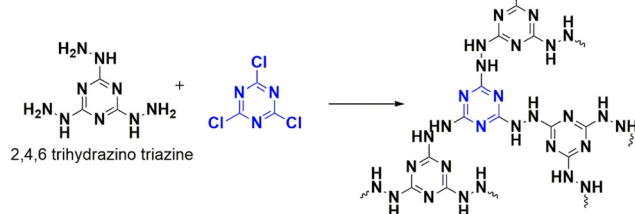


Fig. 18 Scheme for synthesis of CTP-12.

operate at low temperatures, making it suitable for use even in cold-weather countries.

**4.1.1.3. Carbon dioxide utilization.** Carbon dioxide emission impacts the atmosphere in terms of climate change, leading to global warming. It is essential to convert these gaseous molecules into value-added products. The cyclic addition of electrophilic carbon dioxide with basic epoxides generates carbonates, useful intermediates in chemical industries. However, a suitable catalyst is required to perform this reaction.

A breakthrough to mitigate the impact of carbon dioxide emission was achieved in 2018 by Liu *et al.*, who designed a novel hydrazine-linked triazine polymer (CTP-12) that can capture  $\text{CO}_2$  with remarkable efficiency.<sup>64</sup> This polymer was synthesized from nitrogen-rich monomers, cyanuric chloride, and 2,4,6-trihydrazinyl 1,3,5-triazine *via* nucleophilic reaction (Fig. 18). These CTP illustrated amorphous nature existing in aggregate forms. Despite having a low porous nature (pore volume of  $0.28 \text{ cm}^3 \text{ g}^{-1}$ ) and reduced surface area ( $51.2 \text{ m}^2 \text{ g}^{-1}$ ), CTP-12 exhibited an efficiency of  $1.86 \text{ mmol g}^{-1}$  or 8.2 weight (%) in capturing  $\text{CO}_2$  at zero degrees Celsius and 0.1 MPa conditions. This efficiency remained consistent for up to five cycles. One of the significant challenges of converting  $\text{CO}_2$  into valuable substances is its stability and unreactive nature. However, combining it with epoxides can form cyclic carbonates that are synthetically important. CTP-12 is a catalyst that can help in this conversion process when combined with a co-catalyst, tetra-*n*-butylammonium bromide (TBAB), in a solvent-free medium. To optimize this conversion, a model system was used, which consisted of 2-ethyloxirane, CTP-12, and TBAB. Whether the epoxides are terminal or internal, this polymer can catalyze different substrates with various functionalities. This makes CTP-12 an efficient, recyclable, heterogeneous catalyst for carbon dioxide conversion. Hydrazine linkages in this polymer give it a

dual nature, enabling it to adsorb carbon dioxide and activate the epoxides for further conversion.

Dai *et al.* constructed a heterogenous catalyst-based polymer, CTP-13 from cyanuric chloride and phenylene diamine (Fig. 19), which was later modified with a carbonyl-rich imidazolium derivative (CTP-13-IM). The structure of CTP shows a amorphous, flower shaped network with a reduced BET surface area from  $35.4 \text{ m}^2 \text{ g}^{-1}$  to  $16.6 \text{ m}^2 \text{ g}^{-1}$  and a changed pore size from  $14.46 \text{ to } 17.47 \text{ nm}$  due to functionalization. Despite having a low surface area, CTP-13-IM exhibited a comparable adsorption capacity to CTP-13, highlighting the impact of the modification.<sup>63</sup> Additionally, CTP-13-IM had no capture for nitrogen, promoting its selectivity. In the presence of epichlorohydrin (an epoxide), the reaction was catalyzed five times more efficiently by CTP-13-IM than by CTP-13. After optimizing the reaction conditions for catalysis, the polymer-catalyzed reaction proceeded with excellent yields. Electron-withdrawing epibromohydrin and propylene oxide produced the corresponding carbonates with over 90% yield. CTP-13-IM outperformed existing catalysts with five efficiency cycles in short-duration catalysis despite having similar yields in some instances. The nitrogen flanked by two acidic protons in imidazole activates the epoxides towards cyclizing further, directing the reaction.

**4.1.2. Electrocatalyst.** Table 2 lists the CTPs (cyanuric chloride with different linkers) as an effective electrocatalyst with their surface properties.

**4.1.2.1. Nitro reduction and water splitting.** In 2016, Gopi and his co-workers adopted a nucleophilic substitution strategy to build a microporous framework, CTP-13 by selecting triazine-rich cyanuric chloride and benzene 1,4 diamine in an alkaline medium.<sup>77</sup> The framework has a low surface area of  $34 \text{ m}^2 \text{ g}^{-1}$ , likely to be the combination of macropores and mesopores (14.2 nm) (Fig. 19). The filamentous morphology and amorphous pattern characterize the framework. They examined the electrocatalytic activity for synthesized CTP-13: electrocatalytic reduction of nitrobenzene (reduction of toxic nitrobenzene finds a way for its safe disposal and synthesis of other starting materials) and electrochemical oxygen evolution (hydrolytic process) based on cyclic voltammetric studies. The activity is compared with a standard glassy carbon electrode (GC). Regarding the reduction of nitrobenzene, the synthesized framework resembles the performance of the GC electrode. Usually, the oxygen evolution process involves expensive metals like platinum. The modified electrode performed better than the GC electrode but not as the

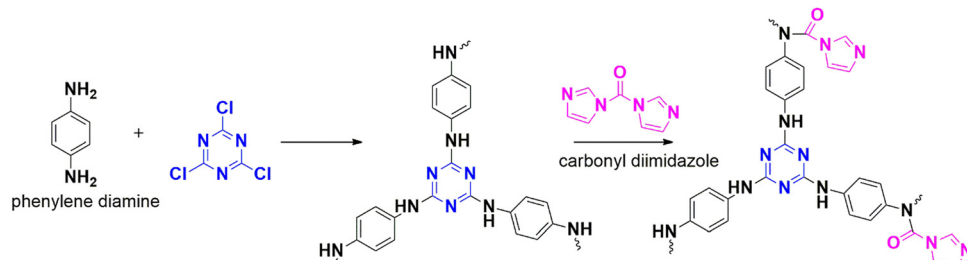


Fig. 19 Scheme for synthesis of CTP-13 and CTP-13-IM.



Table 2 List of CTPs (cyanuric chloride with different linkers) as an effective electrocatalyst with their surface properties

S. No.	CTP	Different linkers	Catalytic reaction	Surface area ( $\text{m}^2 \text{ g}^{-1}$ )	Ref.
1	CTP-13	1,4-Phenylenediamine	Reduction of nitrobenzene Oxygen evolution	34	77
2	CTP-13	1,4-Phenylenediamine	Reduction of nitro compounds Water splitting	32	78
3	CTP-11	Piperazine	Oxygen reduction	578	79
4	CTP-14	Phloroglucinol 1,4-phenylenediamine	$\text{CO}_2$ reduction Water splitting	38	80
5	CTP-15	<i>o</i> -Tolidine	$\text{CO}_2$ reduction Water splitting	>40	81
6	CTP-05	Tetra( <i>p</i> -amino phenyl)porphyrin	Hydrogen generation	311.6	18
7	CTP-16	Phthalocyanine	Sensing of nifedipine by its oxidation	<10	82

metal catalyst. The efficiency of the material can be improved by either carbonizing (enhancing the surface area), composite formation, or adding dopants as a future scope.

In 2022, Rajagopal created an electrocatalyst for water splitting and nitro reduction by CTP-13 (Fig. 19). This was achieved by integrating gold nanoparticles Au@CTP-13, which increased the material stability and directed the catalysis on the metal surface.<sup>78</sup> They synthesized different composites (Au@CTP-13-1 to 4) by varying the chloroauric acid concentration from  $5 \times 10^{-4}$  M to  $2 \times 10^{-3}$  M. These composite structures resembled amorphous graphitic carbon with embedded spherical gold particles, possessing mesopores and a surface area of  $32 \text{ m}^2 \text{ g}^{-1}$ . CTP-10 alone showed no catalytic activity towards nitro reduction, but when incorporated with nanoparticles, it exhibited electrocatalytic activity to reduce 4-nitrophenol and 4-nitroaniline in the presence of  $\text{NaBH}_4$ . The water splitting ability was also evaluated using these gold-embedded polymers in alkaline conditions. In all cases, Au@CTP-13-2 outperformed the other polymers as an efficient electrocatalyst for nitro reduction and water splitting. 4-Nitrophenol and 4-nitroaniline were reduced to corresponding amines within 20 and 14 minutes, respectively. Oxygen and hydrogen evolution was observed at 288 mV and 184 mV overpotential, respectively, at a current density of  $50 \text{ mA cm}^{-2}$ . This efficiency can be attributed to the improved stability and redox active site driving the oxygen generation from peroxide intermediate by lowering the binding energy for hydrogen. The rate is expedited by the faster electron transfer between the gold nanoparticle and polymer. Furthermore, a 2-electrode system using Au@CTP-13-2 was designed to facilitate water splitting and was observed to be stable in an alkaline medium with a current density of  $10 \text{ mA cm}^{-2}$ .

**4.1.2.2. Oxygen reduction.** Chen *et al.* have developed a new catalyst called Co/N-CTP-11, which can replace the expensive platinum catalyst in oxygen reduction conversions (ORR). The CTP-11 catalyst is made by polymerizing cyanuric chloride and piperazine (Fig. 17), then coordinating with cobalt through the basic nitrogen atoms.<sup>79</sup> It is later carbonized to form cobalt-nitrogen-doped porous polymeric sheets. The polymerization resulted in flower shaped sheet morphology with smooth homogeneous macropores, with specific surface areas of  $117 \text{ m}^2 \text{ g}^{-1}$  and pore size of 1.8 nm. Carbonization improved the surface area to  $426 \text{ m}^2 \text{ g}^{-1}$  as in CTP-11-2-900. Pyrrolic

nitrogen is formed during the carbonization, which favors the active binding site for cobalt ions, and pyridinic nitrogen, and graphitic nitrogen, which favors the reduction catalysis. The researchers varied the quantity of cobalt ions and carbonizing temperature, represented by Co/N-CTP-11-*x*-T. They found that Co/N-CTP-11-2-900 had better porous properties and high Co and N contents. In a peroxide-saturated alkaline electrolytic medium, there was an oxygen-reducing peak around 0.79 V, which encouraged further study of Co/N-CTP-11 as an electrocatalyst. The researchers compared the catalytic ability of Co/N-CTP-11-2-900 with the standard expensive platinum/carbon catalyst (Pt/C) often used in oxygen reduction. Co/N-CTP-11-2-900 exhibited a half-wave potential of 0.835 V and a limiting diffusion current density better than the Pt/C catalyst. Furthermore, this reduction reaction is a four-electron-based kinetically controlled reduction. The acid-based catalytic performance of Co/N-CTP-11 was worse than the Pt/C catalyst, but it performed better in a methanol medium with an inevitable tolerance. The uniformly dispersed Co and nitrogen contributed to the superior performance of Co/N-CTP-11 towards ORR.

**4.1.2.3. Carbon dioxide reduction and water splitting.** In 2019, Rajagopal *et al.* developed a polymer-modified glassy carbon electrode (CTP-14/GC) using CTP-14 (Fig. 20), which is made up of cyanuric chloride crosslinked with phloroglucinol and phenylene diamine linkers.<sup>80</sup> This polymer was then carbonized at different temperatures, resulting in CTP-14, CTP-14-500, 700, and 900, with improved surface areas of 38, 93, 201, and  $304 \text{ m}^2 \text{ g}^{-1}$ , respectively. Although carbonization increased the carbon content, it also led to increased disorder and a low porous nature. The materials exhibited an amorphous nature with irregularly shaped morphology. The study evaluated the performance of the material as an electrocatalyst for carboxylation and water splitting. In both cases, the carbonized polymer was found to be better than the normal polymer. In reducing carbon dioxide, the model system 4-bromoacetophenone was considered, which

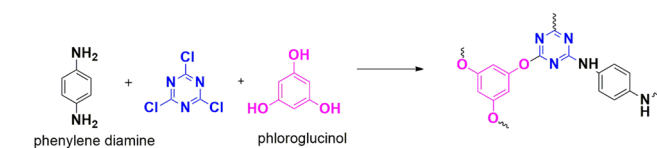


Fig. 20 Scheme for synthesis of CTP-14.



exhibited one reduction wave, where the radical carbanion formed by the reduction of the carbonyl moiety was attacked by  $\text{CO}_2$  to form the corresponding carboxylate anion at a potential of  $-1.27 \text{ V}$  and a current density of  $1.46 \text{ mA cm}^{-2}$ , characteristic to CTP-14-700. For the water-splitting application, CTP-14-900 surpassed other polymers in the hydrogen evolution reaction with an onset potential of  $-0.23 \text{ V}$  at a current density of  $183 \text{ mA cm}^{-2}$ . CTP-14-700 proved better in the oxygen evolution process with an onset potential of  $1.66 \text{ V}$  and a current density of  $148 \text{ mA cm}^{-2}$ . The difference in electrochemical activity is due to the presence of electroactive pyridinic-N, pyrrolic-NH, and quaternary charged nitrogen species, along with a large electrochemically active surface area for CTP-14-700, favoring them for oxygen evolution. Quaternary N is absent in CTP-14-900, where pyrrolic-NH and pyridinic-N are responsible for hydrogen evolution.

In 2022, the same group explored the utilization of metal oxide-incorporated polymers as electrocatalysts in carboxylation and water-splitting reactions. They discovered that copper electrodes can convert propylene oxide to produce the corresponding carbonate by carboxylation.<sup>81</sup> CTP-15 was synthesized from cyanuric chloride and *o*-tolidine (Fig. 21). They also observed that triazine N aids in binding metal ions through coordination. Additionally, CTP-15 was incorporated with oxides of copper, nickel, and mixed copper-nickel nanoparticles. CTP-15 possesses a partially crystalline structure with a graphitic arrangement of atoms and a spherical morphology, while the morphology changes to flaky clusters when decorated with metals such as copper and nickel. The surface properties of the polymers also varied with the addition of metals, with Cu-CTP-15 exhibiting a surface area of  $54 \text{ m}^2 \text{ g}^{-1}$  and Ni-CTP-15 a surface area of  $45 \text{ m}^2 \text{ g}^{-1}$ . Upon assessing the electrocatalytic performance of these polymers for carboxylation and water splitting, it was observed that Cu-CTP-15 demonstrated superior performance for carbon dioxide reduction (with an onset potential of  $-2.18 \text{ V}$  and a current density of  $1 \text{ mA cm}^{-2}$ ) and hydrogen evolution (with an overpotential of  $115 \text{ mV}$  and a current density of  $10 \text{ mA cm}^{-2}$ ). This was attributed to the high surface-to-volume ratio and the availability of active sites due to the oxidation of copper to its oxide form. Conversely, Ni-CTP-15 was found to be a better catalyst for oxygen evolution, exhibiting an overpotential of  $290 \text{ mV}$  and a current density of  $10 \text{ mA cm}^{-2}$ . The presence of a secondary NH group was thought to contribute to this characteristic. Interestingly, the researchers also noted that incorporating mixed metals resulted in moderate behavior in water-splitting reactions.

**4.1.2.4. Hydrogen generation.** Metalloporphyrins are extensively studied as catalysts for hydrogen and oxygen evolution processes.<sup>83</sup> However, owing to low stability and lack of active sites, metalloporphyrins can be integrated into solid polymers to improve efficiency. The generation of hydrogen, our future energy source, is one of the hot topics due to the depletion of fossil fuels.<sup>84</sup> In 2023, Duo *et al.* incorporated N-rich cobalt-based tetra-(*p*-aminophenyl)porphyrin and cyanuric chloride (Fig. 10), forming a triazine polymer CTP-05 for hydrogen generation.<sup>18</sup> As an electron deficit system, cyanuric chloride

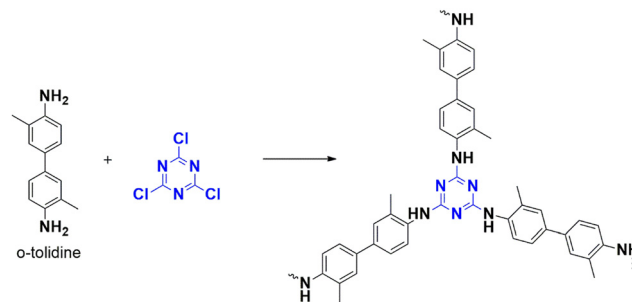


Fig. 21 Scheme for synthesis of CTP-15.

forms an electron donor-acceptor moiety with porphyrin, improving the electronic properties. CTP-05 is characterized by a mesoporous surface (pore size of  $3.6 \text{ nm}$ ) with a large BET area ( $311.6 \text{ m}^2 \text{ g}^{-1}$ ), enhancing the catalytic ability. The particles existed as aggregates of irregular shaped particles. CTP-05 surpasses the existing electrocatalyst by reaching the highest current density of  $10 \text{ mA cm}^{-2}$  within a low over-potential of  $150 \text{ mV}$  and  $210 \text{ mV}$  in acidic and alkaline medium, respectively. Even though the results in the acidic and basic mediums agree regarding a smaller Tafel slope, 100% faradaic efficiency, 10 hours to reach current density, and low charge flow resistance, hydrogen evolution activity is more pronounced in acidic than in the basic medium. Thus, future research will focus on increasing the scalability of other porphyrin-based CTPs for water-splitting protocols.

**4.1.2.5. Oxidation of nifedipine.** Recently, people suffering from high blood pressure have increased, leading to heart diseases and even death. To treat hypertension, doctors often use a drug called Nifedipine, which is an antagonist. Following, a group of researchers led by Liu has developed a new electrochemical sensor (Fig. 22) that uses a unique polymer, CTP-16 made from an electron-rich aluminum-bonded heterocyclic phthalocyanine and an electron-deficient cyanuric chloride.<sup>82</sup> These polymer existed as aggregate particles of uniform distribution (amorphous arrangement) with negligible surface area less than  $10 \text{ m}^2 \text{ g}^{-1}$ . This polymer can effectively detect nifedipine, which has electrochemically active properties due to redox functional groups nitro and dihydropyridine. Phthalocyanines are macrocyclic structures with four N in the isoindole units that can coordinate with different metals, forming complexes with high charge transfer ability. They are usually bridged with electron deficit building blocks like cyanuric chloride to enhance their properties, which can extend to form polymers. The researchers fabricated three different electrodes to compare the efficiency of their work. These included a commercial glass electrode (GE), a modified GE with an aluminum-bridged amine derivative of phthalocyanine (AlTaPc/GE), and a polymer CTP-16/GE. They found that the polymer-derived electrode exhibited the highest current and lowest resistance. The presence of an anode peak and the absence of a peak in reverse scanning indicates that the oxidation of Nifedipine seems to be irreversible (Fig. 23). The oxidation of Nifedipine is the basis of



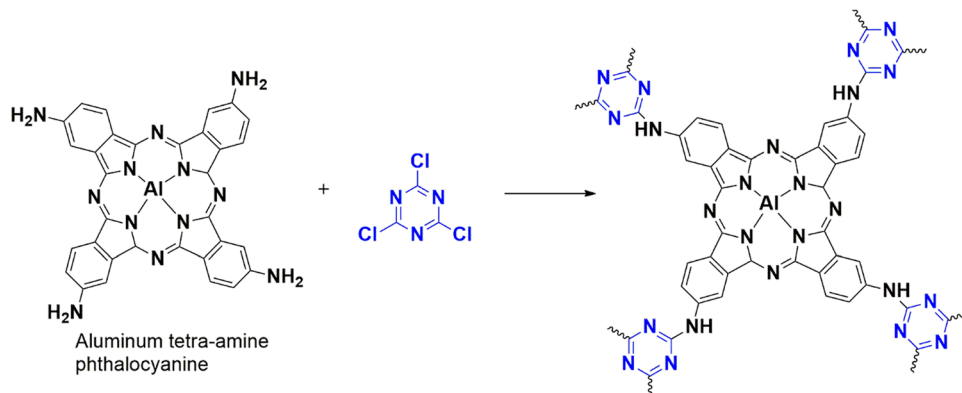


Fig. 22 Scheme for synthesis of CTP-16.

sensing and underscores the CTP-16 electrode's sensitivity and selectivity compared to existing literature.

#### 4.1.3. Photocatalyst

**4.1.3.1. Solar fuel generation.** The level of CO<sub>2</sub> emissions is increasing daily, which can have severe consequences on our environment. Using carbon resources for future fuel is a promising avenue for research. Yadav *et al.* have dedicated efforts to design a new synthetic approach for polymers, CTP-17 (Fig. 24) that involve cyanuric chloride and perylene imide.<sup>85</sup> Structural studies indicated a crystalline nature of sheet-like mesoporous structures of dimensions 3.9 nm. They have also utilized a novel approach by using these CTPs as a photocatalyst for generating solar fuel from carbon dioxide. The ability of perylene as a light harvester is used to mimic naturally occurring photosynthesis. The CTP, along with the monomer synthesized, was coated thrice on a polyimide sheet to generate the thin film of the photocatalyst. To study the efficiency of generating solar fuel, they have compared the ability of the polymer CTP and monomer as photocatalysts based on NADH regeneration and formic acid formation. Surprisingly, the CTP catalyzed better than the monomer, almost four times. This is because of the conjugated electron-rich structure and ordered stacking of the polymer, which endures throughout charge transport. The model system consists of CTP as a photocatalyst and Rh complex, along with NAD<sup>+</sup>, water, and carbon dioxide. The process is initiated with electron excitation in FMO of CTP followed by further transfer to Rh complex. The reduced Rh complex on protonation in water reduces NAD<sup>+</sup> to NADH, thus regenerating NADH. This, in turn, helps formic acid formation from carbon dioxide. They studied the stability of CTP, which may undergo dissociation, forming

formic acid in addition to CO<sub>2</sub>. Supporting this, they experimented with catalyzation without carbon dioxide. They even performed the reaction without CTP, without a source of sunlight, without Rh complex, and NAD<sup>+</sup>. In all the cases, no formic acid formation was observed, which agrees with the stable nature of CTP. They obtained more than a 96% yield for formic acid and the regeneration ability of NADH, with three cycles of reusability. This opens the future scope of the ability of CTPs as a photocatalyst.

**4.1.3.2. Aerobic oxidation.** A group led by Wu recently designed a metal-free catalyst for photolytic aerobic oxidation of benzylamine and sulfides that form sulfoxides and imines, which are crucial for synthetic reactions.<sup>86</sup> The catalyst was generated from cyanuric chloride and polarizable bipyrazoles of benzene, furan, and thiophene, named CTP-18, CTP-19 and CTP-20 (Fig. 25). The as-made polymer was composed of porous graphitic (flakes) structure with amorphous nature. The goal of this work is to enhance the absorption of visible light by introducing extended conjugation with characteristic band gaps. Incorporating bipyrazole derivatives adds to its dipole moment, which can alter optical and electronic properties with efficient charge separation and transfer. The photocatalytic performance of thioanisole and benzylamine was studied, and it was found that CTP-20, which is rich in thiophene, exhibited better photocatalytic activity due to its high degree of polarization, resulting in charge separation and transfer. In addition to this, CTP-20 has a high ability to generate reactive oxygen species (superoxides and singlet oxygen) with small energy of dissociating electron-hole pairs into mobile charge carriers. CTP-20 can be reused with comparable activity for three cycles.

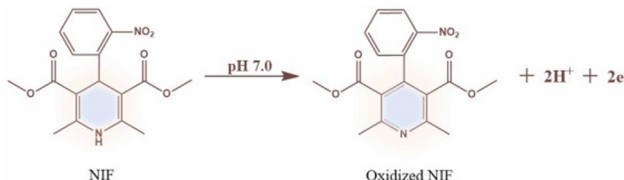


Fig. 23 Plausible oxidation mechanism of nifedipine (NIF) at pH 7.0. Adapted from ref. 82 Copyright 2024 Elsevier.

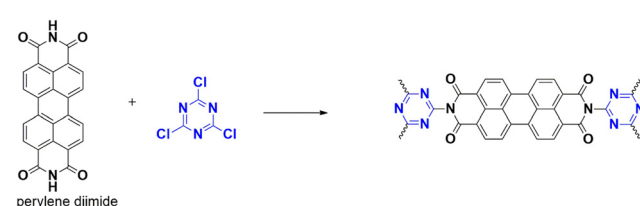


Fig. 24 Scheme for synthesis of CTP-17.



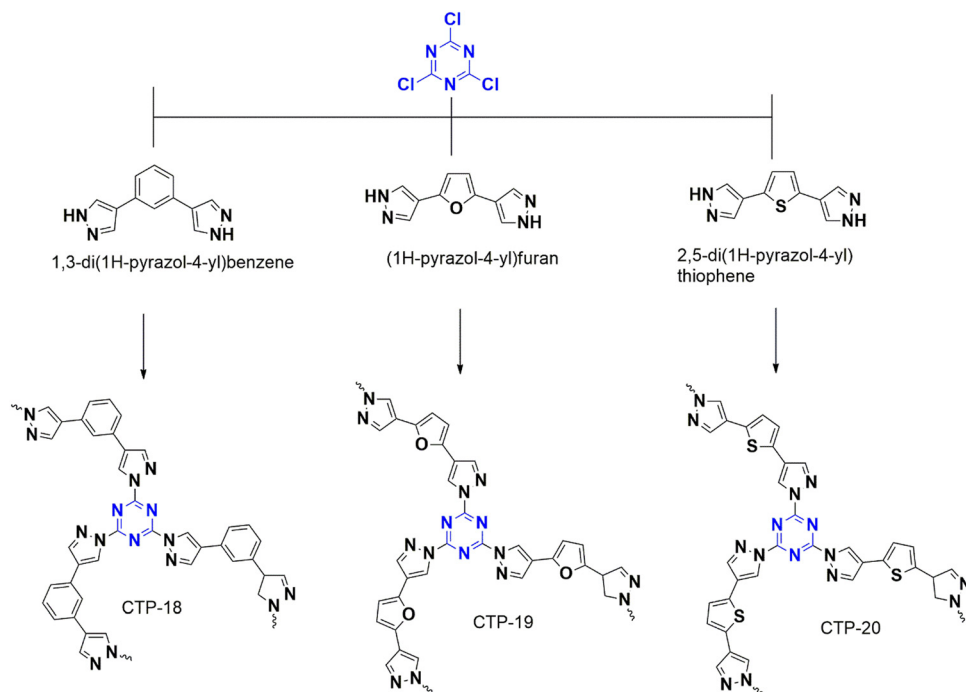


Fig. 25 Scheme for synthesis of CTP-18, CTP-19, and CTP-20.

#### 4.2. Pollutant removal

Table 3 lists the different CTPs having cyanuric chloride as the scaffold, along with their adsorption capacity towards different pollutants in the environment and surface area.

Rapid urbanization and industrialization result in discharging pollutants into water, which has no other substitutes. These pollutants vary from inorganic contaminants like heavy metal ions and radioactive nuclides to organic pollutants like dyes, pesticides, and aromatic hydrocarbons.<sup>3</sup> They are highly soluble, non-biodegradable, and persist in our environment. They are highly toxic and induce harmful effects on living organisms.<sup>96</sup> On the other hand, available fresh water is scarce. Finding a suitable material for removing these pollutants from water is challenging. Recently, porous materials have been widely used for this application.

**4.2.1. Removal of organic pollutants.** Detoxification of colorless and odorless fumigants in agricultural production is rarely reported compared to other pollutants. Tang *et al.* have developed a wearable detoxifying CTP to remove these toxic carcinogenic fumigants.<sup>87</sup> CTP-06 was made from cyanuric chloride and melamine (Fig. 12) and was nucleophilically grown on a cotton fiber (SAFE-cotton) for practical applications. The CTP prepared by this method possesses a high specific surface area ( $598.2 \text{ m}^2 \text{ g}^{-1}$ ;  $6.07 \text{ nm}$ ), good stability, and amorphous ordered spherical particles. To test the effectiveness of CTP, they used methyl iodide as a representative fumigant and compared the performance of cotton fiber, SAFE-cotton, and CTP-06. Surprisingly, both CTP-06 and SAFE-cotton performed similarly, achieving equilibrium within 1 minute. No adsorption was observed for pure cotton fiber. The experiment was extended to other fumigants, which also showed similar

results. Further analysis of methyl iodide in all concentrations was studied. It was found that SAFE-cotton adsorbs less than CTP-06, with storage for up to 1 day. An observable color change (pale yellow-brown) was also noted during adsorption. The nucleophilic basic N in CTP-06 and the alkylation of triazine N by fumigants play a role in detoxification. The reusability of CTP-06 was also demonstrated, as it could be used for up to five cycles.

Kojo *et al.* undertook a study to create a new polymer by combining cyanuric chloride and polycyclic aromatic systems, namely anthracene and phenanthrene. This polymer was later modified by introducing amide and imine functionalization by oxidation, resulting in two different polymers (Fig. 26): CTP-21 and CTP-22.<sup>88</sup> Modifying the polymer increased the interplanar spacing and surface polarity, making it an ideal adsorption material. Both the CTP was analyzed with amorphous nature. Both CTP-21 ( $768 \text{ m}^2 \text{ g}^{-1}$ ) and its oxidized form ( $660 \text{ m}^2 \text{ g}^{-1}$ ) existed as rectangular aggregates whereas CTP-22 ( $165 \text{ m}^2 \text{ g}^{-1}$ ) and its oxidized form ( $93 \text{ m}^2 \text{ g}^{-1}$ ) as spherical aggregates. To test the effectiveness of the new polymer, the emerging pollutants, bisphenol A, bisphenol S, and naphthol, were selected. The results showed that both polymers could adsorb the pollutants better than existing adsorbents. Interestingly, CTP-21 performed better than CTP-22 despite the latter having higher surface properties. Naphthol was found to be the most easily absorbed out of the selected pollutants. They found that the CTPs exhibited four times reusability with a chemisorbed interaction with a 1:1 complexation between the adsorbent and adsorbate. The adsorption was mainly due to the  $\pi$ - $\pi$  interaction and H bonding possibility endured by imine nitrogen and amide oxygen (Fig. 27). Overall, these CTPs have the

**Table 3** List of different CTPs of cyanuric chloride along with their adsorption capacity towards different pollutants in the environment and surface area

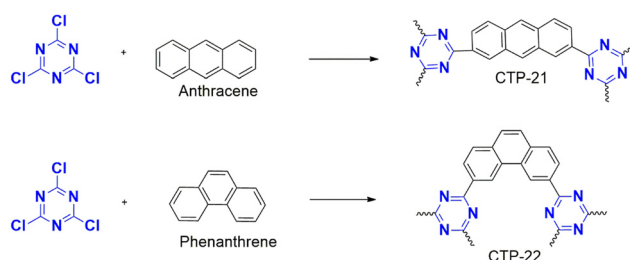
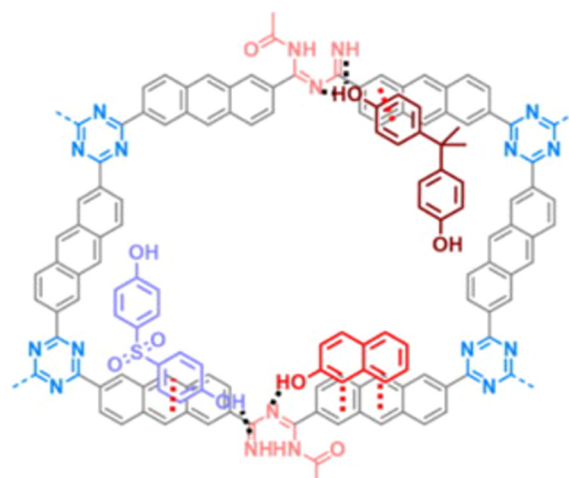
S. No.	CTP	Different linkers	Adsorbate	Adsorption capacity (mg g <sup>-1</sup> )	Ref.
1	CTP-06	Melamine	Methyl iodide	596.88	87
2	CTP-27	(Trimidazolyl phenyl)amine	Oxoanions (chromate, rhenium oxide)	396, 441.6	3
3	CTP-21	Anthracene	Dyes (methyl orange)	300	
	CTP-22	Phenanthrene	Bisphenol A	247	88
			Bisphenol S	249	
			Naphthol	376	
4	CTP-06	Melamine	Dyes (Congo red)	1581	89
5	CTP-11	Piperazine	Isopropanol	165	90
	CTP-23	Spiro linker			
6	CTP-11	Piperazine	Rhodamine B	153	91
7	CTP-28	Triphenyl methane	Basic blue 41	631	53
			Basic red 46	580	
8	CTP-06	Melamine	Direct scarlet 4 BS	215.28	5
9	CTP-24	Spiro fluorene	Benzene/cyclohexane	878	92
	CTP-25	Triptycene		441	
	CTP-26	Phenyl derived adamantane			
10	CTP-29	Carbazole derivative	Iodine vapour	4.6 g g <sup>-1</sup>	93
			Iodine from cyclohexane	293 mg g <sup>-1</sup>	
11	CTP-30	Trihydrazinotriazine	Iodine from cyclohexane	340	94
		Perylene 3,4,9,10 tetracarboxylic dianhydride			
12	CTP-31	Tris(4-aminophenyl)amine	Iodine vapour	4.62 g g <sup>-1</sup>	95
13	CTP-32	Diphenyl acetylene	Iodine vapour	5.12 g g <sup>-1</sup>	47
			Iodine from <i>n</i> -hexane solution	667 mg g <sup>-1</sup>	

potential to be further exploited for other pollutants due to their excellent adsorption capabilities.

Isopropanol is a type of volatile organic compound (VOC) that is considered an emerging pollutant. It is extensively used in semiconducting semiconductors, making it a significant environmental concern. To tackle this issue, Lu and his team led a study synthesizing a triazine-rich polymer CTP-23 using a mixed linker protocol made from cyanuric chloride, linear piperazine, and nonlinear spiro molecules (Fig. 28) as linkers.<sup>90</sup> They utilized multiple linkers to break the regular stacking of polymers, which improved the surface properties and exposed the binding sites, allowing for better interactions. Two types of polymers were synthesized, namely CTP-11 from cyanuric chloride and piperazine (Fig. 13) and CTP-23 by incorporating both linkers. BET results showed that CTP-11 had a low surface area ( $302.3 \text{ m}^2 \text{ g}^{-1}$ ) but better carbon dioxide adsorption capacity than CTP-23 ( $458.8 \text{ m}^2 \text{ g}^{-1}$ ). CTP-23 had larger pores (1.2–2 nm), which reduced the effective interaction of gas compared to CTP-11. The particles existed in aggregate forms with amorphous ordering. Five VOCs, including isopropanol at 800 and 1000 ppm concentrations, were tested for their adsorption performance. The adsorption primarily depended on the molecular diameter, polarity, and extent of hydrogen bonding. At 800 ppm, toluene was found to be better

adsorbed than the other VOCs due to its larger diameter, which fit well in the pores of the polymer. At 1000 ppm, isopropanol was found to be better adsorbed due to its hydrogen bonding ability. The polymer developed can be reused up to five times, making it an excellent solution for semiconductor hubs. This study highlights the importance of incorporating spiro derivatives to improve adsorption.

Separating benzene/cyclohexane mixtures poses a significant challenge for chemical industries due to their similar boiling temperatures and the formation of azeotropes. However, these molecules are critical in various reactions as they are the primary starting materials. Therefore, it is imperative to develop effective adsorption and separation techniques. In this regard, Yan *et al.* have designed a polymer for this purpose that

**Fig. 26** Scheme for synthesis of CTP-21 and CTP-22.**Fig. 27** Adsorption mechanism of CTP-18 towards the organic pollutants: bisphenol-A, bisphenol-S, and naphthol. Adapted from ref. 88 Copyright 2022 Elsevier.

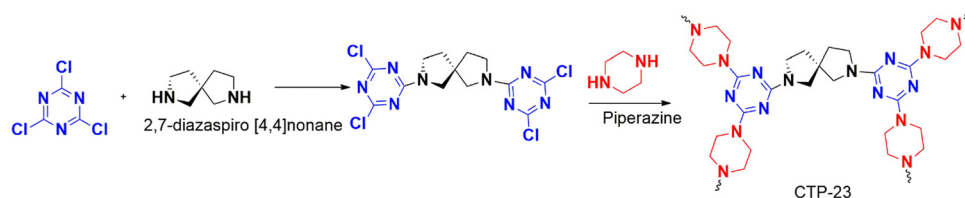


Fig. 28 Scheme for synthesis of CTP-23.

is synthesized from cyanuric chloride (Fig. 29) combined with spiro fluorene, triptycene, and phenyl derivatives of adamantane, which are labeled as CTP-24, 25, 26 respectively.<sup>92</sup> The polymerization resulted in amorphous nature with aggregation of rough surface spherical particles. CTP-24 and CTP-25 exhibited micropores with surface area of 371 and 452 m<sup>2</sup> g<sup>-1</sup> with pore dimensions of 0.7 and 0.56 nm. CTP-26 possessed both micro and mesopores (1 nm and 4 nm) with surface area of 154 m<sup>2</sup> g<sup>-1</sup>. To investigate the adsorption behavior of this polymer, the researchers employed a sorption isotherm and examined a benzene/cyclohexane/helium mixture. The results showed that all CTPs exhibited better benzene uptake than cyclohexane, attributed to the  $\pi$ - $\pi$  interaction between the polymer and the aromatic benzene, which is substantially less in non-aromatic cyclohexane. Furthermore, the critical temperature (T<sub>c</sub>) was crucial in this process. Benzene, having a higher T<sub>c</sub> than cyclohexane, was significantly adsorbed. Nevertheless, the uptake of both vapors was more refined than that reported in previous studies. Regarding vapor uptake, CTP followed CTP-24 > CTP-25 > CTP-26. This phenomenon can be due to the decrease in pore volume from CTP-24 to 26 due to a reduction in the number of aromatic systems, including

triazine and benzene. They also studied the selectivity of the vapors and found that CTF-26 > CTF-25 > CTF-24. This surprising result can be attributed to the decrease in molecular volume from the spacious adamantane system to the sterically hindered spiro fluorene.

**4.2.2. Removal of oxoanions and dyes.** Neutral POPs are more explored than charged POPs for different applications. In 2021, Jiao *et al.* introduced the concept of quaternization for developing a charged CTP (CTP-27) from cyanuric chloride and tri(imidazolyl phenyl)amine (Fig. 30), followed by the addition of benzyl bromide for inducing charge to the polymer.<sup>3</sup> Presence of hierarchical pores was identified with surface area of 274 m<sup>2</sup> g<sup>-1</sup> and amorphous nature. The quaternization of N in the polymer enhanced the surface potential, as evidenced by zeta potential data. Thus, anions are more likely to interact strongly with polymers through electrostatic force. At higher pH, interaction reduces due to negative surface potential. The adsorptive capacity of oxo-anions was investigated with Cr<sub>2</sub>O<sub>7</sub><sup>2-</sup>, ReO<sub>4</sub><sup>-</sup>, and MnO<sub>4</sub><sup>-</sup> along with interfering anions. Interestingly, adsorption was least affected by interfering anions, and CTP-27 has selectivity towards MnO<sub>4</sub><sup>-</sup>. Three anionic dyes, including methyl blue, cargo red, and methyl

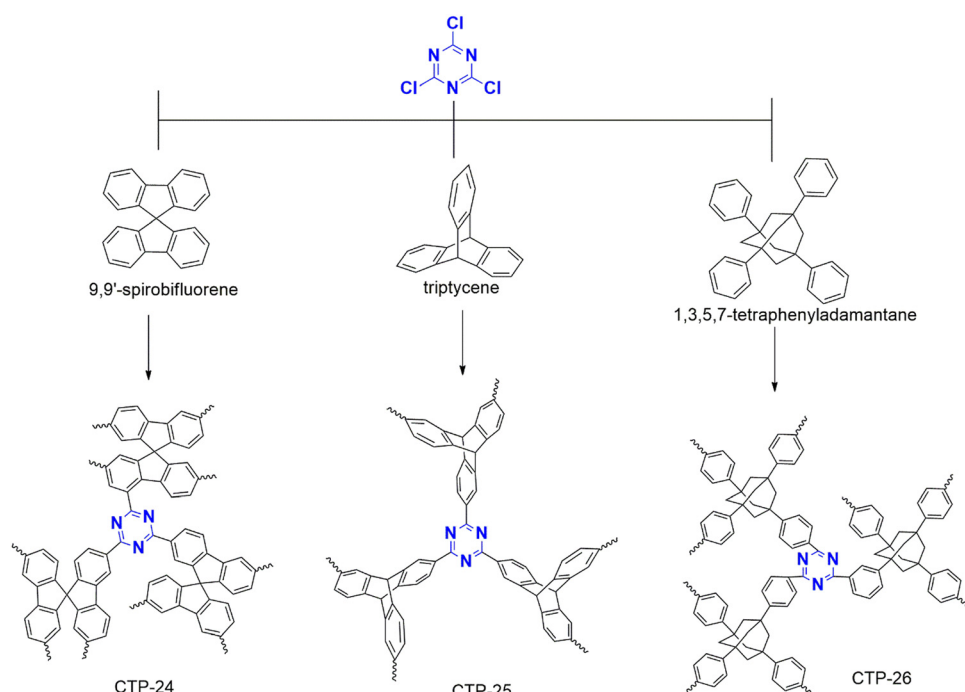


Fig. 29 Scheme for synthesis of CTP-24, CTP-25, CTP-26.



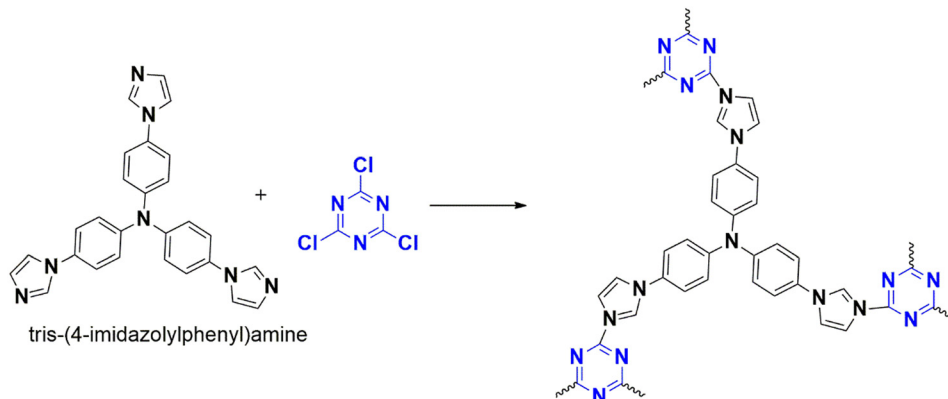


Fig. 30 Scheme for synthesis of CTP-27.

orange, were considered, along with cationic dyes (methylene blue, rhodamine B). Anionic dyes (preferably methyl blue and Congo red) were adsorbed to a greater extent than cationic dyes. Adsorption of anionic pollutants is directly correlated with the temperature of the medium. pH of the solution was lowered after adsorption due to the exchange of  $\text{Cl}^-$  and  $\text{Br}^-$  in the pores. CTP-27 exhibits better adsorption (single-layer Langmuir isotherm) than the reported polymer, which can be reused for three cycles. Adsorption of the polymer revolves around the ion-exchanging capacity of pore-filled  $\text{Cl}^-$  and  $\text{Br}^-$ , strengthened by electrostatic forces. Besides, the pollutant's charge and size (volume occupied) affect the ion exchange. Thus, CTP-27 has a distinctive ability to adsorb both oxoanions and anionic dyes from water, which is rarely reported in the literature.

The researchers Wu *et al.* have created a porous polymer, known as CTP-06, using affordable reactive monomers, cyanuric chloride, and melamine, (Fig. 12) capable of adsorbing cationic and anionic dyes.<sup>89</sup> These amorphous porous material possessed a surface area of  $670 \text{ m}^2 \text{ g}^{-1}$  with pore distributed at 1.2 nm. The adsorption phenomenon occurs due to the basic nature of nitrogen, triazine N, and amino N, as well as H bonding, which interacts with the acidic interacting sites in the anionic dyes. To produce different polymers, the researchers carbonized CTPs at various temperatures. They also fabricated CTP into an aerogel CTP-06/PVDF@MF, where CTP-06 is dispersed into PVDF and suspended in melamine foam (MF) at varying concentrations to produce different aerogels. The researchers found that the CTP-06 exhibited remarkable efficiency in removing anionic dyes, especially Congo Red, compared to cationic dyes, with Rhodamine B being one of the best cationic dyes. The adsorption phenomenon occurs due to the H donor-acceptor bonding and electrostatic interaction, which plays a significant role in all pH conditions. The researchers performed further in-depth studies on adsorption, which revealed that both dyes were chemisorbed multilayer with a high affinity for Congo red. They found that size was less significant in adsorption, with Congo red, which is bulkier than Rhodamine B, showing better adsorption. These findings underscore the impressive capabilities of the CTP in dye removal, which is a significant contribution to the field. Further, the cooperative effect of anionic dyes on cationic dye adsorption was analyzed,

and it was found that cationic dyes showed enhanced interaction in the presence of Congo Red. The CTP prefers Congo red, which can further interact with cationic dyes. Adsorption of Congo red reduces the charge on the CTP surface, which can kindle the interaction towards cationic dyes. The effect of annealing of CTP on adsorption was also studied, with symmetrizing amino N into triazine systems reducing the adsorption capacity of anionic dyes. They were able to regenerate the CTP six times with comparable results. Further studies of the application of aerogel in adsorption found that it exhibited better efficiency towards anionic dye pollutants, with better adsorption when large amounts of CTP were dispersed. The findings of this study suggest that CTPs can help remove cationic and anionic dyes from wastewater.

Sanjabi *et al.* synthesized a CTP-11 from cyanuric chloride and piperazine<sup>91</sup> in 2023 (Fig. 17). These flower-shaped nanosheet structures was characterized with porous surface of  $154.6 \text{ m}^2 \text{ g}^{-1}$  and size less than 50 nm and partial crystallinity. The polymer was more than 70% efficient in removing different dyes from water (Fig. 31). Specifically, adsorption characteristics (isotherm and kinetic study) for removing Rhodamine B were studied. The adsorption matched with the modified Langmuir-Freundlich model and fractal-like pseudo-first-order model, indicating the heterogeneity of the material. The reusability of the material was investigated (5 cycles), and it was observed that adsorption capacity decreased. The material was effective in removing dyes from industrial wastewater with the advantage of effective removal in neutral pH under room conditions.

Taheri *et al.* designed and synthesized a triazine polymer, CTP-28 using cyanuric chloride and triphenyl methane through the Friedel-Crafts reaction in 2024 (Fig. 32). The resultant polymer was post-functionally sulfonated with chlorosulfonic acid and named CTP-28- $\text{SO}_3\text{H}$ .<sup>53</sup> CTP exhibited amorphous nature with surface area changed from  $137.4$  to  $50.15 \text{ m}^2 \text{ g}^{-1}$  due to sulfonation. The researchers evaluated its adsorption ability towards two cationic textile dyes, Basic blue 41 and basic red 46 (Fig. 33). CTP-28- $\text{SO}_3\text{H}$  efficiently removed these dyes from aqueous media compared to unmodified CTP-28 due to the abundant binding sites in the polymer contributed by sulphonyl groups. Kinetic studies suggest that the polymer



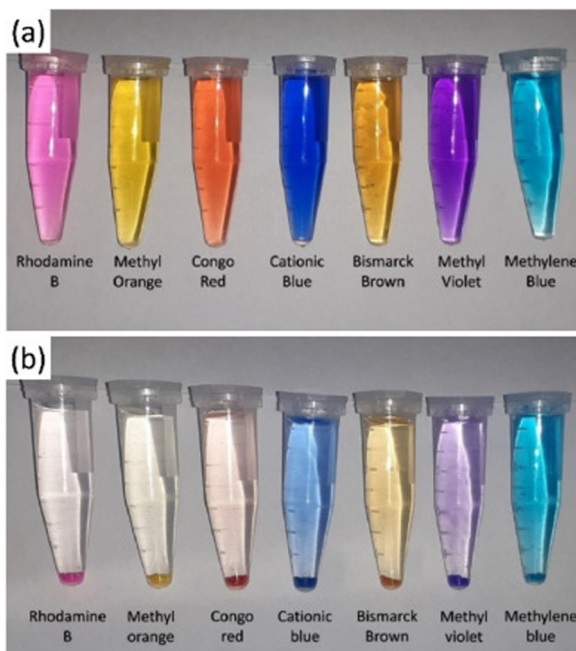


Fig. 31 Changes during the adsorption before (a) and after (b) of different dyes by CTP-11. Adapted from ref. 91 Copyright 2023 Elsevier.

follows either a pseudo-second-order or pseudo-first-order model. The Langmuir isotherm model confirms the monolayer adsorption ability from the thermodynamic studies. The adsorption behavior is mainly contributed by the interaction sites in the polymer from aromatic systems and sulphonyl groups, facilitated by  $\pi$ - $\pi$  interaction, H bonding, and electrostatic attraction between the dyes and the polymer. CTP-28- $\text{SO}_3\text{H}$  can be reused for three cycles and is superior to existing polymers in removing these dyes.

Tadayoni and his team developed a magnetic porous adsorbent to remove Direct Scarlet 4BS, a widely used carcinogenic dye in industries. Their approach involved coating iron oxide nanoparticles on silica to create a magnetic core, which was then functionalized with amine to react with cyanuric chloride.<sup>5</sup> The free ends of chlorine reacted with melamine (as in Fig. 12), and diamine-derived ethane was used to ensure the complete conversion of chlorine atoms, resulting in MNP@m-CTP-06. Structural analysis proved the CTP to be spherical aggregates of porous particles (surface area of  $11.39 \text{ m}^2 \text{ g}^{-1}$  with  $1.21 \text{ nm}$  pores) with amorphous morphology.

After optimizing the adsorption conditions, MNP@m-CTP-06 effectively adsorbed the anionic dye Direct Scarlet 4BS. At an acidic pH of 3, MNP@m-CTP-06 removed the dye with 94% accuracy compared to other adsorbents, following non-linear kinetics that supported more diffusion-based adsorption (Fig. 34). The dye was physically adsorbed onto the surface according to the Konda isotherm model, indicating the presence of two binding sites, one more active than the other. The binding property could be attributed to the combined effects of electrostatic interaction and hydrogen bonding. The presence of functionalized binding sites (hydroxyl, azo, etc.) on the dye favored its effective removal and was recycled for four turns.

**4.2.3. Iodine capture.** Nuclear energy is emerging as a promising alternative fuel. However, nuclear power is generated through radioactive nuclide disintegration, including long-life nuclides like iodine and its isotopes, which pose risks to humans and the environment. To mitigate these risks, it is crucial to eliminate these nuclides, which can be accomplished using porous polymers. Polymers that contain electron-rich heteroatoms and a conjugated aromatic structure are essential for adsorbing acidic iodine. Besides these, iodine is widely used in healthcare to detect thyroid infections and screen displays. So, capturing and reusing this iodine can reduce its environmental impact.

Xu and his team have explored a new approach of using polymers to capture iodine. They have also developed a way to use the captured iodine to sequester carbon dioxide, contributing to global warming.<sup>93</sup> The researchers synthesized three polymers containing a carbazole moiety: CTP-29-RT, and CTP-29. CTP-29-RT was developed by linking the carbazole monomer at room conditions (Fig. 35). In contrast, different CTP-29 were created by changing the reaction conditions with cyanuric chloride as the crosslinker. It exhibited hollow structure with surface porosity of  $640 \text{ m}^2 \text{ g}^{-1}$  and micropores distributed over 0.7 and 1.3 nm. Room temperature conditions reduced the surface area to  $422 \text{ m}^2 \text{ g}^{-1}$ . CTP-29 is unique in its ability to capture iodine vapor ( $4.6 \text{ g g}^{-1}$ ) and iodine solution ( $293 \text{ mg g}^{-1}$ ) and is hollow in nature with high nitrogen contributed by carbazole and cyanuric chloride with carboxyl functionalization (during the hydrolysis of carbazole moiety) followed by C-CTP-29 and CTP-29-RT. The polymers can also catalyze the conversion of carbon dioxide to carbonates due to their high nitrogen content. The captured iodine acts as a co-catalyst for the cycloaddition of the carbon source, resulting in high yields. Epichlorohydrin was chosen to optimize catalytic activity. The iodine adsorbed as polyiodide ions can interact with the polymer, converting carbon dioxide to carbonates. The polymers follow the order of CTP-29 > C-CTP-29 > CTP-29-RT in both the capturing of iodine and the conversion of carbon dioxide. They can be reused for up to three cycles with considerable efficiency.

Recently, a porous polymer, CTP-30, was developed by Esmaeilikhani *et al.* from the monomers 2,4,6-trihydrazino-1,3,5-triazine and perylene-3,4,9,10-tetracarboxylic dianhydride.<sup>94</sup> The trihydrazinotriazine monomer was synthesized using hydrazine and cyanuric chloride (Fig. 36). The CTP-30 polymer has a porous structure (nanorods with surface area of  $475 \text{ m}^2 \text{ g}^{-1}$  and

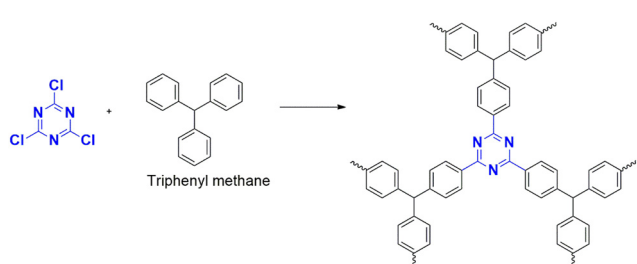


Fig. 32 Scheme for synthesis of CTP-28.



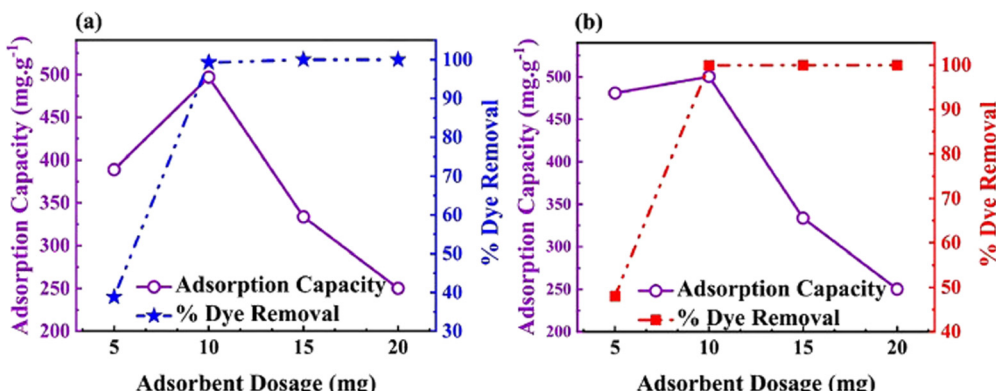


Fig. 33 Representation of adsorption capacity and dye removal efficiency of sulfonated CTP-28 towards different dyes (a) basic blue 41 and (b) basic red. Adapted from ref. 53 Copyright 2023 Elsevier.

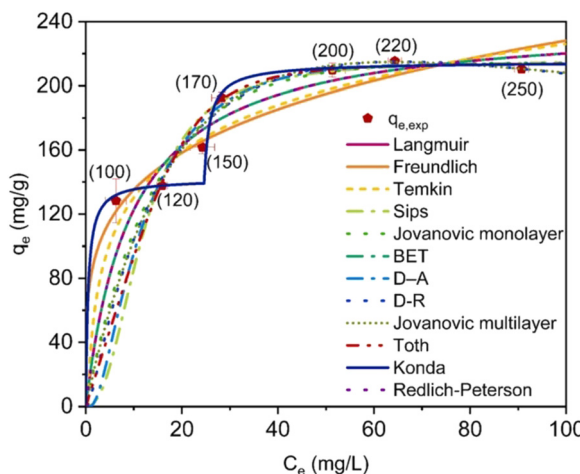


Fig. 34 Representation of different isotherms exhibited by MNP@-CTP-06 towards DS-4BS. Adapted from ref. 5 Copyright 2023 Elsevier.

micropores at 1.64 nm) with semicrystallinity, and the presence of perylene reinforces its stability rings with aromatic conjugation. This makes it effective in adsorbing iodine, which is electron-rich with heteroatoms. The adsorption isotherm studies follow the Langmuir model with a monolayer interaction with iodine. CTP-30 has excellent adsorption properties towards iodine from a

cyclohexane solution (340 mg g<sup>-1</sup>) in three hours, outperforming existing materials. The polymer can be reused for up to four cycles. Iodine adsorption can occur *via* physisorption or chemisorption. The porous nature of CTP-30 allows it to capture iodine through physisorption. At the same time, chemisorption occurs due to the formation of a charge transfer complex between iodine and the functional groups in CTP-30, such as phenyl, -NH, and imine linkages.

A polymer, CTP-31 was developed by Wang *et al.* that can capture iodine (Fig. 37) by polymerizing trifunctionalized cyanuric chloride and aminophenyl-derived amine.<sup>95</sup> The polymer was analysed with sheet-like, amorphous structure with characteristic high surface area of 328 m<sup>2</sup> g<sup>-1</sup> and mesopores over 3.84 nm. The technique of gravimetric analysis was used to study the application. Over 10 hours, the polymer had an adsorption capacity of 4.62 g g<sup>-1</sup> for gaseous iodine due to the interaction of iodine and polyiodide ions with basic nitrogen and conjugated phenyl systems. A color change was observed, indicating the diffusion of iodine into the pores of the polymer. The material also exhibited a good retention capacity, allowing it to store iodine and capture it. The removal capacity of iodine from cyclohexane and aqueous phase was also investigated. The adsorption behavior in a liquid system was characterized by multilayer chemisorption. The mechanism can be explained as follows: the iodine molecules are physisorbed into the pores and then converted to

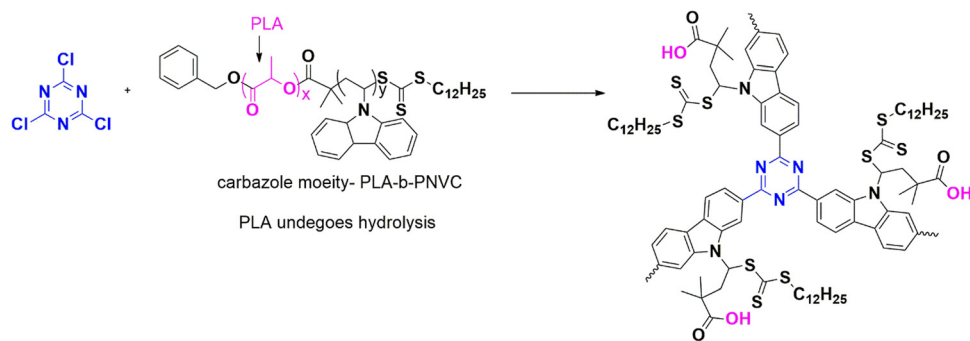


Fig. 35 Scheme for synthesis of CTP-29.



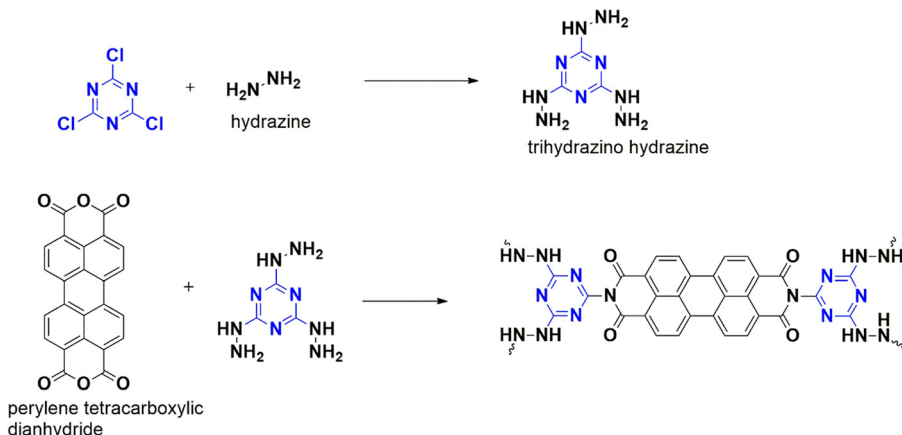


Fig. 36 Scheme for synthesis of CTP-30.

corresponding polyiodides facilitated by charge transfer complexation with the polymer functionalized with phenyl system and heteroatoms.

Pourebrahimi *et al.* developed and synthesized a porous polymer to capture iodine using the Friedel–Crafts mechanism with cyanuric chloride.<sup>47</sup> They also used ethyne-derived diphenyl (DPA) as the other monomer for the adsorbent (Fig. 38). The resulting polymer possess sheet-like 2D structures and large surface areas ( $943 \text{ m}^2 \text{ g}^{-1}$  and pores at  $2.49 \text{ nm}$ ) with amorphous nature. This polymer, CTP-32 showed the highest adsorption performance for iodine in a vapor state and from a solution (hexane). The researchers compared its performance with an analog adsorbent CTP-34 with trans-stilbene (TS),

ethene linked to phenyl rings (Fig. 40). CTP-32 ( $5.12 \text{ g g}^{-1}$ ) showed better capacity in both gaseous and hexane media than CTP-34 ( $3.75 \text{ g g}^{-1}$ ). Both adsorbents could be reused for up to five cycles while retaining their adsorption ability. The efficiency of the adsorbent can be attributed to its high surface properties, high N hetero effect that enables better acid-based interactive binding, and rich conjugated  $\pi$  systems that promote electrostatic interactions. The possibility of charge transfer is also responsible for the adsorption. It is better to adsorb iodine from the gaseous phase ( $667 \text{ mg g}^{-1}$ ) than from the liquid phase since the vapor interaction happens at high temperature, and there is a possibility of solvents getting trapped in the porous adsorbent in the liquid phase. Surprisingly, most of the iodine penetrated the pore in the form of molecular iodine rather than polyiodide form. Therefore, CTP-32 seems to be a better adsorbent for iodine and radio-nuclear waste than the existing polymers.

#### 4.3. Solid phase extraction

To separate and extract different compounds, the technique of microextraction in the solid phase (SPME) is widely employed. The extraction process relies on the relative distribution of the pollutant between the sample solution and the fiber coating to ensure effective extraction. The role of the fiber coating is pivotal in this process. For example, accurately detecting drugs and other metabolites in the human body is critical to legal investigations and medical treatment. Recently, researchers have utilized a microextraction technique involving thin films created through the electrospinning method to conduct this analysis.<sup>97</sup>

Samira and her team have successfully developed a nanofilm composite comprised of cellulose (CNC), a hydroxy-rich polysaccharide, and a polymer known as CTP-33.<sup>98</sup> The CTP-33 polymer is synthesized from cyanuric chloride and an amino derivative of naphthalene (Fig. 39), while the film is strengthened with polyethylene glycol. The formed polymer possessed a certain degree of order of spherical nanoparticles uniformly distributed with a surface area of  $4.5 \text{ m}^2 \text{ g}^{-1}$ . Both the polymer and CNC contain ample functionalization to extract suitable molecules. In evaluating the

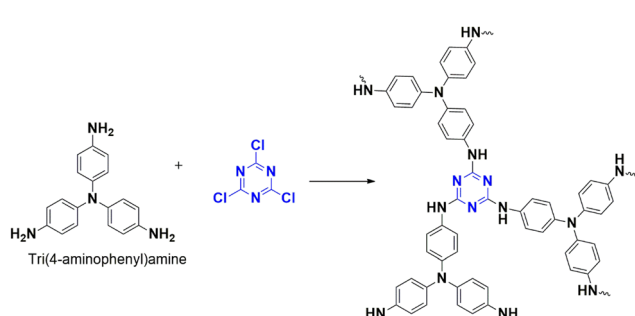


Fig. 37 Scheme for synthesis of CTP-31.

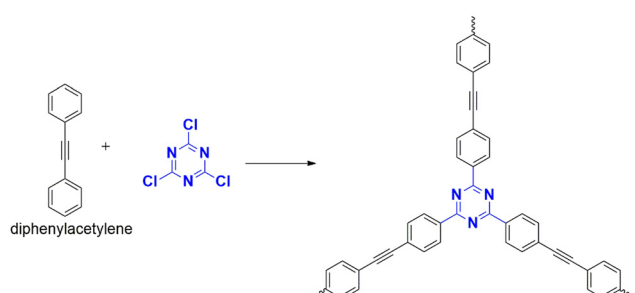


Fig. 38 Scheme for synthesis of CTP-32.



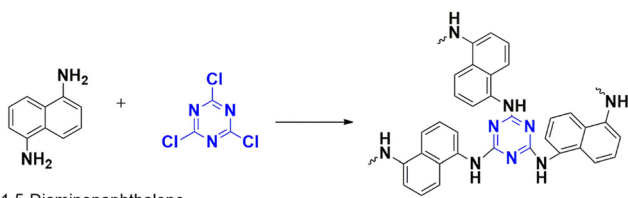


Fig. 39 Scheme for synthesis of CTP-33.

thin film's efficacy as a microextractor of imipramine, an antidepressant, the presence of aromatic rings, basic amino groups, and hydroxyl groups played a pivotal role in extraction through hydrogen bonding and pi-pi interaction. The nanocomposite film outperformed individual units of CNC and commercially used cellulosic paper.

Polyyclic aromatic hydrocarbons (PAH) and their oxygenated and nitrogenated derivatives are a group of emerging pollutants known for their malignant nature. A recent study conducted by Wang *et al.* focused on the design and synthesis of an extraction fiber from porous polymer CTP-34, which was later fabricated onto a stainless steel aided by silicone.<sup>10</sup> CTP-34 is formed by polymerizing cyanuric chloride with the *trans* isomer of stilbene (Fig. 40). They exhibited amorphous ordering of sheet like structure with surface area of  $919 \text{ m}^2 \text{ g}^{-1}$  and pore size of 2.54 nm. The researchers studied the extraction efficiency of the fiber for polyaromatic hydrocarbons and their oxygen and nitrogen derivatives. The CTP-34-based fiber is rich

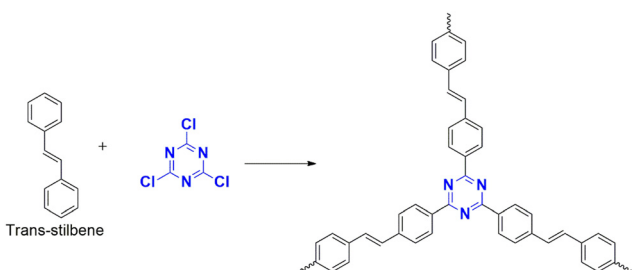


Fig. 40 Scheme for synthesis of CTP-34.

in conjugation, making pi-pi interaction a possible reason for its efficient extraction. As the degree of conjugation increases from naphthalene to anthracene, the extraction capacity of the fiber improves. It was observed that PAH exhibited better extraction from the mixture than their derivatives, which can be attributed to hydrophobic interaction. The researchers also conducted real water analysis and found that the CTP-34-based fiber was more effective than the reported ones.

Chen *et al.* developed an organic-inorganic porous polymer, CTP-35 by introducing a new concept of improving the availability of binding sites to enhance its applications (Fig. 41). To achieve this, they introduced a sterically hindered monomer to prevent stacking arrangement.<sup>99</sup> Cyanuric chloride and bulky building block POSS-P (an oligomer of silsesquioxane with phenyl rings) were selected for this purpose. Due to steric reasons, stacking layering is reduced, exposing the available active sites for different interactions. It was analysed with a nano-networked smooth structure with poor crystallinity. Different frameworks (CTP-35-*xy*, *x*, and *y* are molar ratios of monomers) were synthesized by varying the ratios of the building blocks, followed by heating to high temperatures to form CTP-35-*xy*-C/Si. Heating reduces the pore characteristics along with the active binding sites. CTP-35-161 possessed the highest surface area of  $578 \text{ m}^2 \text{ g}^{-1}$ . Due to better porosity of CTP-35-81 (surface area of  $464 \text{ m}^2 \text{ g}^{-1}$ ), the polymer with 8 moles of cyanuric chloride and 1 mole of POSS-P was selected for further studies. Both CTP-35-81 and CTP-35-81-C/Si were used as the fiber coating in SPME to enrich benzene derivatives. CTP-35-81 exhibited better results than the heated polymer due to the decrease in available sites for interaction. Of all the benzene derivatives, the xylene derivative was enriched effectively.

A recent study led by Weng and their team resulted in the development of an extraction membrane designed to enrich endocrine-disrupting nitrophenols and their derivatives (Fig. 42). The membrane comprises a composite PAN@CTP-36, created by first developing a amorphous polymer CTP-36 using cyanuric chloride and triphenyl phosphane *via* the Friedel-Craft mechanism.<sup>100</sup> The polymer was then grown *in situ* on polyacrylonitrile (PAN) fiber to form the extraction membrane, confirming

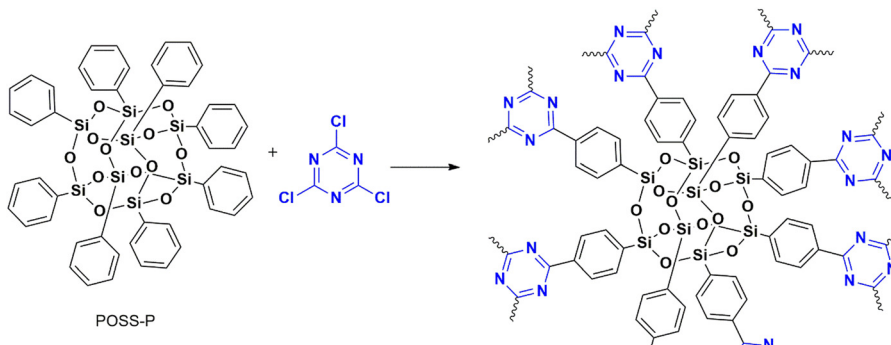


Fig. 41 Scheme for synthesis of CTP-35.



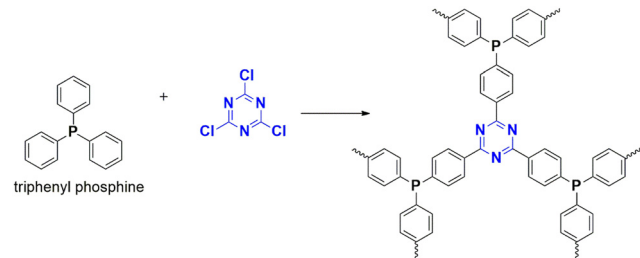


Fig. 42 Scheme for synthesis of CTP-36.

formation by using various techniques. SEM analysis confirmed the color change of the particles from white to brown on incorporating the CTP-36 on to PAN. After investigating the extraction performance of individual PAN, CTP-36, and PAN@CTP-36 towards different nitrophenols (Fig. 43), it was observed that the PAN@CTP-36 unit performed the best. The team then optimized various parameters and found that this composite membrane could efficiently enrich the respective pollutant even at minor concentrations. This is due to the combined effect of hydrogen bonding, hydrophobic effects, and  $\pi$ - $\pi$  interaction, which are contributed by the chemical nature of the composite. Real water analysis was conducted to study the membrane's practical applicability for removal.

Phthalate esters (PAEs) are commonly used in plastics and food packaging films to provide flexibility and elasticity. However, elevated levels of PAEs have been found in humans and can interfere with biological functioning. To address this issue, Wang *et al.* used a technique called extraction using a coated stirring bar (SBSE), followed by HPLC, to detect phthalate esters and their derivatives.<sup>101</sup> The researchers utilized porous polymer CTP-37 to coat the stir bar (Fig. 44), which was developed from cyanuric chloride and amine terphenyl derivative. The polymer formed is amorphous with rough surfaced particles having a porous surface area of  $56.3 \text{ m}^2 \text{ g}^{-1}$ . After optimizing the extraction conditions, CTP-37 was evaluated and compared

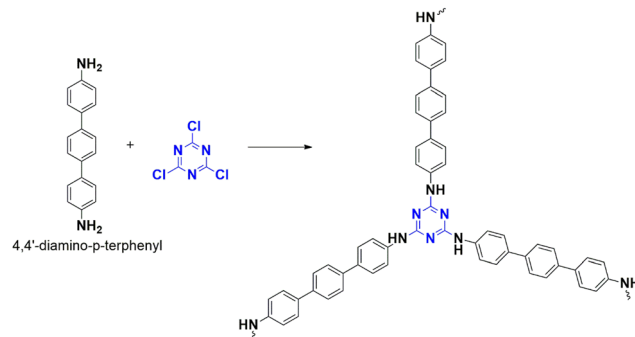


Fig. 44 Scheme for synthesis of CTP-37.

to existing extractors. The performance of CTP-37-coated bars was better than that of commercial extractors, likely due to the abundance of conjugating phenyl rings and basic nitrogen that interacted with the sample matrix through  $\pi$ - $\pi$  interaction, hydrophobicity, and hydrogen bonding. While the performance of HPLC using CTP-37-coated bars was lower than that of existing membranes, it was higher than that of extraction based on mass spectrometry. The researchers analyzed mineral water and liquor samples. They detected two PAEs, diethyl and dibutyl phthalates, in mineral water, but no esters were found in the liquor samples.

Nitrobenzene is a significant intermediate for many valuable products available in the market. However, it can also be found to be a pollutant with carcinogenic toxicity in water sources. To extract nitrobenzene and its aromatic derivatives (NBS) in SPME, Chang *et al.* developed an amphiphilic hypercross-linked polymer, CTP-38, from lipophilic cyanuric chloride with pyridine (Fig. 45).<sup>102</sup> CTP-38 polymeric particle exhibited an amorphous nature with irregular flake-like structure. They were characterized with a surface area of  $371 \text{ m}^2 \text{ g}^{-1}$  and pores distributed at 3.8 nm. The extraction was followed by flame ionization coupled with gas chromatography. The researchers fabricated this polymer into a fiber coating for the extraction protocol. Since nitrobenzene is polar, the researchers utilized suitable polar adsorbents to enrich it. After optimizing the extraction conditions, the CTP-38 could extract NB from water with low detection limits and high enrichment (Fig. 46). Among the pollutants, dimethyl-derived nitrobenzene exhibited better performance. The chemically stable SPME fiber can be repeatedly used without losing its efficiency. Possible interactions may occur due to electron-rich polymers and electron-deficit nitro groups, resulting in donor-acceptor interactions. This

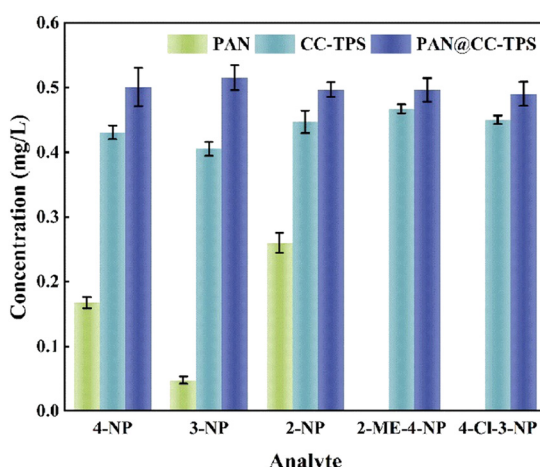


Fig. 43 Extraction of nitrophenol derivatives by PAN, CTP-36(CC-TPS) and PAN@CTP-36 (PAN@CC-TPS). Adapted from ref. 100 Copyright 2024 Elsevier.

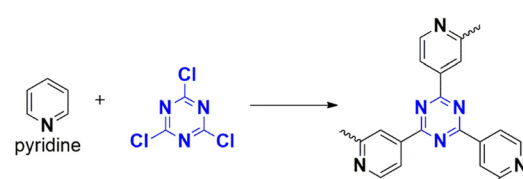


Fig. 45 Scheme for synthesis of CTP-38.

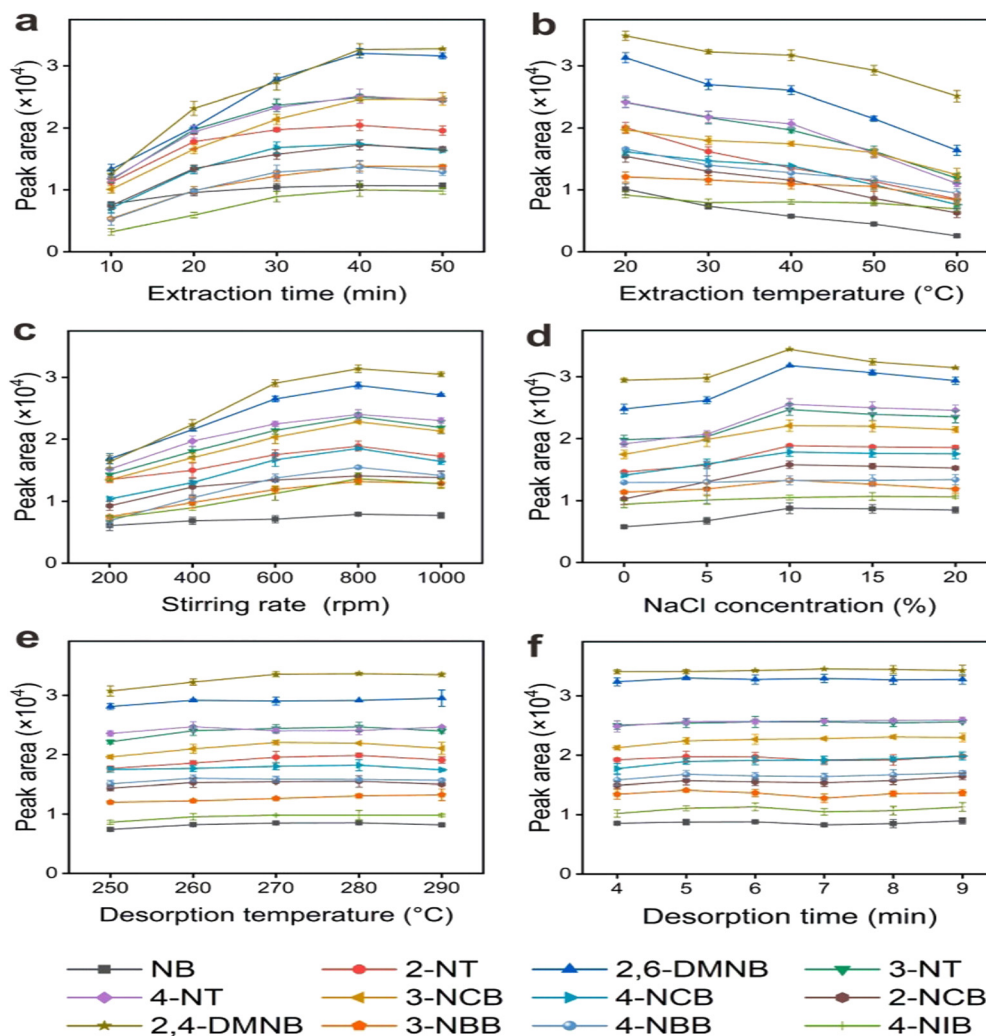


Fig. 46 Optimization of different parameters towards extraction of nitroaromatic compounds by CTP-38. Adapted from ref. 102 Copyright 2023 Elsevier.

polymer, CTP-38, outperforms existing fibers and adsorbents for removing nitro compounds.

#### 4.4. Gas adsorption and separation

List of different CTPs from cyanuric chloride with their carbon dioxide uptake capacity and surface area is listed in Table 4.

Carbon dioxide, a greenhouse gas, accumulates in the atmosphere due to increasing energy requirements from burning fossil fuels, eventually leading to global warming. Being the primary component of natural gas, they can solidify and corrode the pipelines irrespective of being inert.  $\text{CO}_2$  levels must be standardized for the better usage of natural gases. Earlier alkanol amines<sup>25</sup> were used in excess quantity for their

Table 4 List of different CTPs from cyanuric chloride with their carbon dioxide uptake capacity and surface area

S. No.	CTP	Linkers	Surface area ( $\text{m}^2 \text{ g}^{-1}$ )	Gas uptake	Ref.
1	CTP-03	<i>p</i> -Terphenyl	553	$33 \text{ cm}^3 \text{ g}^{-1}$	103
2	CTP-40	Tetraphenyl ethene	1200	$216 \text{ mg g}^{-1}$	42
	CTP-41	Tetraphenyl silane	523	$152 \text{ mg g}^{-1}$	
3	CTP-13	1,4-Phenylene diamine	—	$0.67 \text{ mmol g}^{-1}$	2
4	CTP-11	Piperazine	88.5	$0.9 \text{ mmol g}^{-1}$	104
5	CTP-42	Styrene derivative	1266	$141 \text{ mg g}^{-1}$	105
6	CTP-13	1,4-Phenylene diamine	20.6	$0.4 \text{ mmol g}^{-1}$	4
	CTP-13-NH		18	$0.56 \text{ mmol g}^{-1}$	
7	CTP-43	4,4'-Bis( <i>N</i> -carbazolyl)-1,1'-biphenyl	579	12.66 wt%	106
8	CTP-44	Tetraphenyl-1,4-phenylene diamine	883	12.98 wt%	107

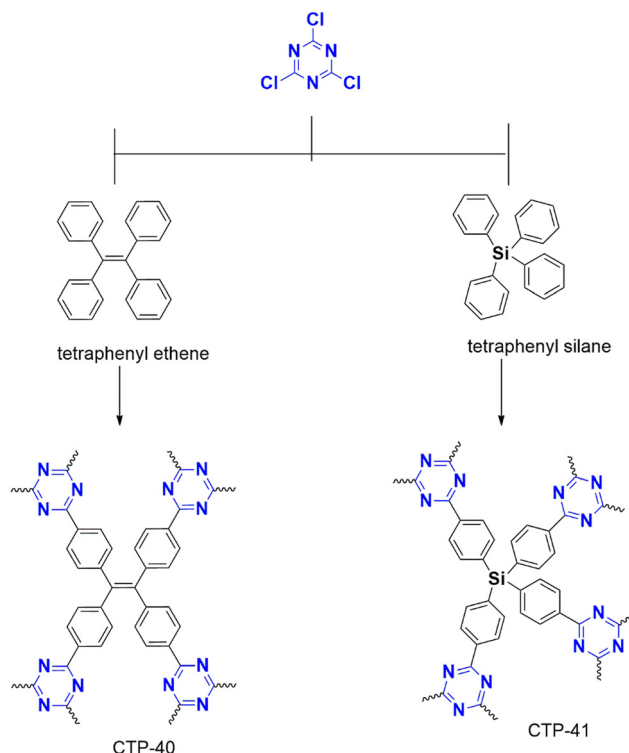


Fig. 47 Scheme for synthesis of CTP-40 and CTP-41.

separation, which suffered from difficulty in regeneration. Now, researchers are developing porous materials that can adsorb these gases. Cheap synthesis, selectivity of gases, and low

energy regeneration are necessities for such materials.<sup>2</sup> Introducing NH functionality in the polymer improves the selectivity of CO<sub>2</sub>-N<sub>2</sub> and CO<sub>2</sub>-CH<sub>4</sub> gases.<sup>108</sup> Aromatic rings enhance the surface properties and temperature stability.<sup>109</sup>

Meng *et al.* created a membrane using a polymer enriched with cyanuric chloride and aromatic *p*-terphenyl (CTP-03). The membrane was later reinforced with polysulfone (CTP-03/PSF) to improve its strength.<sup>103</sup> The as-made polymer was composed of spherical-shaped uniformly distributed particles and a desirable BET surface area (553.4 m<sup>2</sup> g<sup>-1</sup>) with hexagonal pores at 1.2 nm. The polymer and membrane were tested for their ability to adsorb and separate gaseous carbon dioxide and nitrogen. Due to the abundance of nitrogen (Fig. 7), which is responsible for dipolar interactions and van der Waals forces, the gases diffuse into the pores. CTP-03 can accommodate more CO<sub>2</sub> than N<sub>2</sub> due to the less polarized nitrogen atoms. This makes it an effective tool for selective and efficient separation of gases. The matrix membrane can also exhibit the same properties, performing even better than CTP-03. The researchers also studied the effect of CTP-03 composition, pressure, and temperature on adsorption. Increasing the CTP-03 content increased adsorption property and separation due to better interaction with CO<sub>2</sub> than N<sub>2</sub> with increasing nitrogen atoms. The pressure effect was the same for adsorbing CO<sub>2</sub> and N<sub>2</sub> gases. However, at higher pressure, the separation decreased due to better diffusion of N<sub>2</sub> than CO<sub>2</sub>. Adsorption of CO<sub>2</sub> remained unaffected by temperature, whereas N<sub>2</sub> adsorption improved. This reduced the separation effect of both gases. This indicates that the membrane is highly stable across

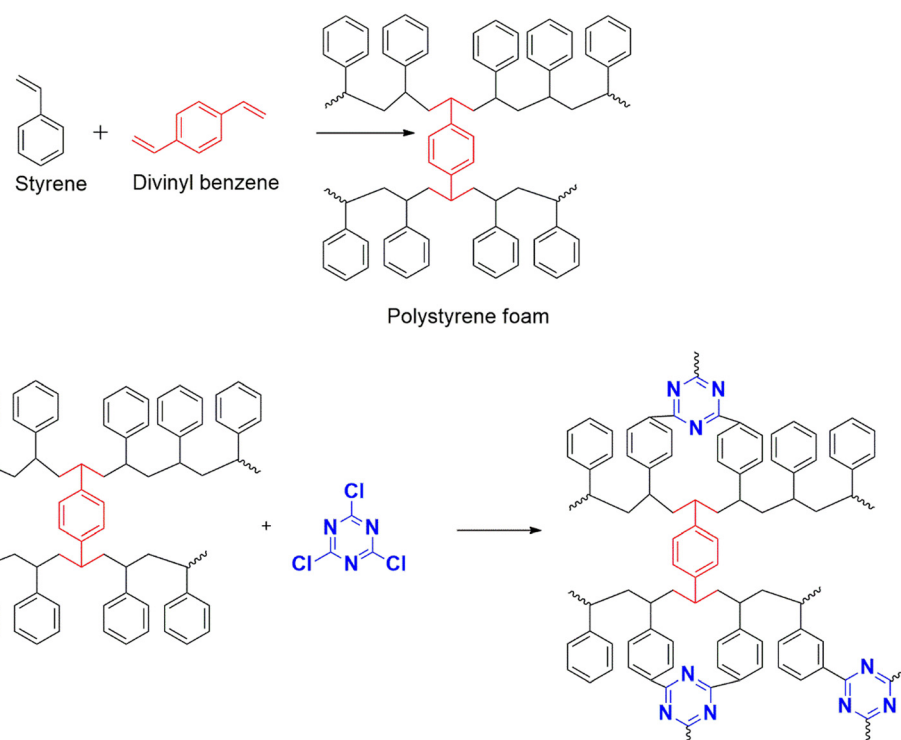


Fig. 48 Scheme for synthesis of CTP-42.

various temperatures and pressures. The polymeric matrix is also durable, retaining its robustness for up to eight days.

Later, Puthiaraj *et al.* designed and developed two polymeric adsorbents using cyanuric chloride and tetraphenyl carbon and silane derivatives – CTP-40 and CTP-41, respectively (Fig. 47). CTP-41 had less nitrogen content due to the bulky building block, silane, which hindered complete polymerization.<sup>42</sup> Both the polymers exhibited amorphous nature with aggregation of spherical particles. Nitrogen ratio and surface properties (micropores at 1.2–1.3 nm) play a significant role in carbon dioxide adsorption. Silicon content in CTP-41 deprived the basic nature of nitrogen, which reduced its carbon dioxide capture capacity. Therefore, CTP-40 (216 mg g<sup>-1</sup>; 1200 m<sup>2</sup> g<sup>-1</sup>) was better than CTP-41 (142 mg g<sup>-1</sup>, low surface area of 523 m<sup>2</sup> g<sup>-1</sup>) and other reported adsorbents. The polymeric adsorbents displayed enhanced selective carbon dioxide capture over other gases, such as nitrogen and methane. CTP-40 was efficient in both capture and selective adsorption compared to other systems. Additionally, it could store carbon dioxide (528 mg g<sup>-1</sup>) and methane (37 mg g<sup>-1</sup>) with eight turns of reusability.

In 2017, Lee *et al.* reported a porous triazine polymer (CTP-13) from cheap building blocks, cyanuric chloride, and 1,4-phenylenediamine<sup>2</sup> by simple nucleophilic reaction (Fig. 19). More information on the structural and porosity is not performed by the researchers. They studied the adsorption capacity of carbon dioxide during the post-combustion process and compared the results with polymer CTP-11 (cyanuric chloride and piperazine; Fig. 17). CO<sub>2</sub> is chemisorbed to the surface due to interaction with the NH group. CTP-11 (0.85 mmol g<sup>-1</sup>) exhibited better CO<sub>2</sub> uptake than CTP-13 (0.67 mmol g<sup>-1</sup>), which is attributed to the weak interaction of amino moieties towards CO<sub>2</sub> in CTP-13 due to resonating aromatic rings. CTP-13 gets saturated better than CTP-11, even though the sorption process is irreversible. CTP-13 exhibited better adsorption compared to aliphatic diamine polymers. Regeneration is poor in this material due to chemisorbed gas molecules, which cannot be desorbed as expected.

The same group constructed a CTP-11 (Fig. 17) from cyanuric chloride and piperazine by metal-free nucleophilic substitution in 2018.<sup>104</sup> They have focused on its ability to adsorb carbon dioxide from natural gas (as methane) under atmospheric parameters instead of post-combustion. CTP-11 has a

reasonable surface area (88.5 m<sup>2</sup> g<sup>-1</sup>) with petal-shaped morphology. These petal-like particles aggregate into a bulky spherical shape, which restricts the diffusion of gas molecules owing to low surface properties (mesopores at 9.7 nm). CO<sub>2</sub> sorption isotherm reflects that these molecules occupy the mesopores at low partial pressure. On increasing pressure, adsorption rises due to the clustering of molecules and occupancy in these mesopores. The absence of hysteresis indicates the physisorption of CO<sub>2</sub> with a low value of heat of adsorption, minimizing energy usage for regeneration of the adsorbent. The material exhibits a selectivity in adsorbing CO<sub>2</sub> (0.9 mmol g<sup>-1</sup>) over CH<sub>4</sub> (0.1 mmol g<sup>-1</sup>). This selectivity is due to the interaction between electron-rich adsorbent and oxygen atom owing to its high quadrupole moment.<sup>110</sup>

Hierarchical porous polymers are a class of polymers with many different types of pores, including macropores, micro pores, and mesopores. Duan *et al.* developed nitrogen-rich polymers (CTP-42) from cyanuric chloride.<sup>105</sup> Styrene and divinylbenzene were polymerized using a free radical mechanism to create a microporous polystyrene foam matrix. Later, cyanuric chloride was added using a Friedel–Crafts reaction to create meso- and micropores (Fig. 48). The molar ratios of styrene, divinylbenzene, cyanuric chloride, and DCM solvent were varied to create different CTP-42 (CTP-42-1 to CTP-42-9). CTP-42-6 had the highest surface area (1266 m<sup>2</sup> g<sup>-1</sup>) of all the CTP-42s'. CTP-42 are better at adsorbing carbon dioxide at room temperature than other porous polymers. This could be important for developing more efficient and sustainable carbon capture technologies. The researchers looked at the effect of nitrogen content and porous properties on adsorption. They found that micropore volume had the most significant influence on adsorption, followed by surface area and nitrogen content. CTP-42-6 had the highest surface area and microporous volume, making it the best adsorbent among the CTP-42s. At lower temperatures, CTP-42-6 had a greater capacity for adsorption with low adsorption heat values, meaning it had good physisorption properties and could be regenerated. CTP-42-6 also had a higher selectivity for carbon dioxide over nitrogen gas.

In 2020, Mukhtar *et al.* reported the synthesis of triazine polymer from the monomers cyanuric chloride and 1,4-phenylene diamine (Fig. 19) by nucleophilic reaction protocol forming CTP-13.<sup>4</sup> It was later modified with monoethanolamine,

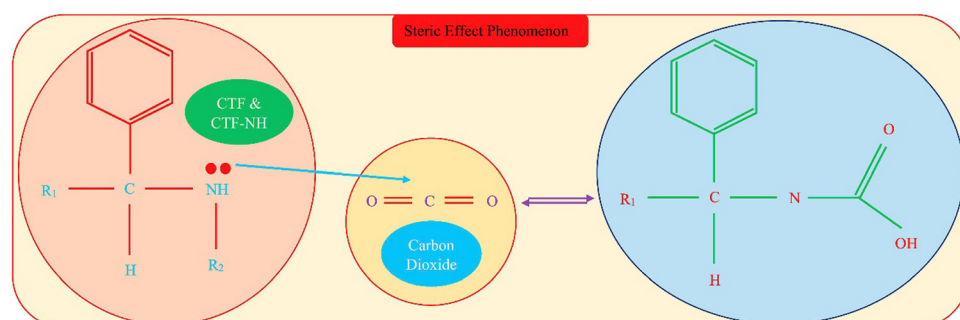


Fig. 49 The steric effect leading to lower adsorption of CO<sub>2</sub>. Adapted from ref. 4 Copyright 2020 Elsevier.



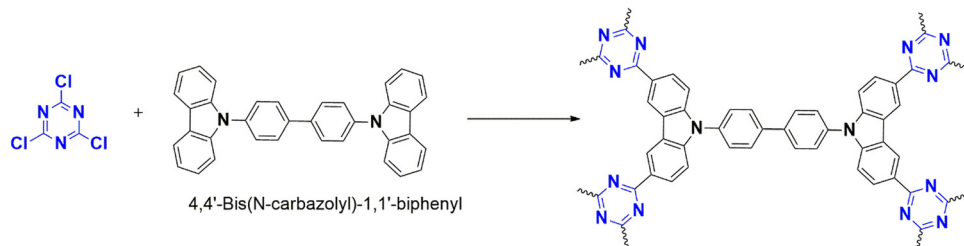


Fig. 50 Scheme for synthesis of CTP-43.

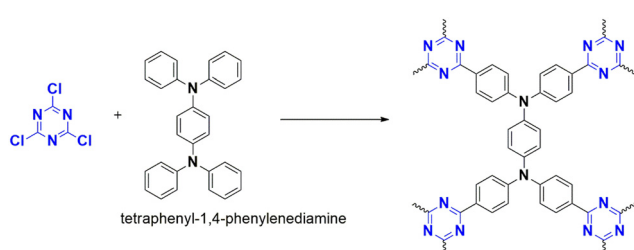


Fig. 51 Scheme for synthesis of CTP-44.

commonly used for  $\text{CO}_2$  capture, forming CTP-13-NH. These amorphous polymers exhibited a decrease in surface area from  $20.61 \text{ m}^2 \text{ g}^{-1}$  on functionalization. Both the polymers were characterized and studied for their ability to adsorb carbon dioxide and selective adsorption of  $\text{CO}_2$  and  $\text{CH}_4$ . Although modifications reduced the surface area, they increased the N content of these stable polymers, which, along with the presence of electron-deficient triazine rings, is essential for interaction with acidic  $\text{CO}_2$  (Fig. 49). These polymeric structures are enriched with ultra micropores, which are better suited for high carbon dioxide adsorption than nitrogen and methane due to structural diameters. Even in low-pressure regions, carbon dioxide adsorption is highly pronounced, strengthened by amine functional groups and ultramicro porosity. The modifications have enhanced the gas capture by 40% compared to CTP-13, which agrees with the adsorption study. The selectivity of  $\text{CO}_2$  over  $\text{CH}_4$  has increased by 30% in CTP-13-NH compared to CTP-13 due to the poor interaction of non-polar methane molecules with the polymer. Thus, CTP-13-NH can purify natural gas better than the reported combinations with a high surface area. This narrows down the concept of surface area being less significant for carbon dioxide capture.

Sadak and his team have successfully developed three different types of polymers using carbazolyl (YBN) fixed core treated with various linkers such as dimethoxy methane (YBN-DMM), dimethoxybenzene (YBN-DMB), and cyanuric chloride (CTP-43; Fig. 50). CTP-43 existed as amorphous, aggregate particles with surface area of  $579 \text{ m}^2 \text{ g}^{-1}$  and ultramicropores (0.57 nm) and mesopores (5.86 nm). They have conducted extensive research to study the impact of changing the linkers on capturing and storing different gases.<sup>106</sup> The results of the research indicate that the adsorption of carbon dioxide decreases as the temperature increases. Among the three

polymers, the methoxy methane-derived polymer (YBN-DMM) performs best due to the size matching of the pores and carbon dioxide. Although all the polymers have almost similar  $\text{CO}_2$  capture capacity, CTP-43 exhibits high  $\text{CO}_2$  affinity as it contains essential nitrogen electron density. The trend of decreased adsorption with an increase in temperature is also observed for gaseous nitrogen, methane, CO, and oxygen. YBN-DMM performs better than the other two polymers, followed by CTP-43 and YBN-DMB, respectively. The thermodynamic calculations predicted the physical adsorption of gaseous molecules, which reduces the energy consumption for the durability of the polymers. CTP-43 exhibits better adsorption of hydrogen among the three polymers due to the presence of nitrogen atoms. Additionally, with increasing temperature, CTP-43 has better selectivity for  $\text{CO}_2$  than other gases, followed by YBN-DMM and YBN-DMB. This can be attributed to the abundant triazine system with nitrogen atoms. The research demonstrates that YBN-DMM is the most effective polymer for capturing and storing gases, but CTP-43 had better selectivity.

Later, the same research group led by Cucu *et al.* designed a protocol to use tetraphenyl-derived phenylene diamine (TPPA) instead of a fixed core moiety like carbazole (Fig. 51). The TPPA was treated with dimethoxymethane (DMM), dimethoxybenzene (DMB), and cyanuric chloride (CC) following the Friedel-Craft mechanism.<sup>107</sup> The result was three porous polymers: TPPA-DMM, TPPA-DMB, and CTP-44. These amorphous aggregated polymeric particles exhibited ultramicropores at 0.57 nm along with pores at 2.05 nm and surface area of  $742 \text{ m}^2 \text{ g}^{-1}$ . When exploring the carbon dioxide capture capability, it was found that the adsorption decreased with an increase in thermal conditions, which agreed with previous results. The lower interaction between the polymer and gas may have been due to resonance stabilization. In the last study, TPPA-DMB, with high surface properties, exhibited better gas adsorption than YBN-DMM. However, at 320 K, CTP-44 surpassed other polymers with a unique adsorption ability. Dimethoxy benzene derived polymer (TPPA-DMB) had higher carbon dioxide, nitrogen, oxygen, and CO uptake at higher temperatures. However, due to the abundant nitrogen atoms responsible for H bonding, CTP-44 enhanced its adsorption for methane and hydrogen even at high temperatures. TPPA-DMM selectively adsorbs carbon dioxide over nitrogen, whereas TPPA-DMB has selectivity over methane, oxygen, and CO. But at higher temperatures, CTP-44 improved its selectivity over oxygen, and CO. A trend of decrement in the properties was observed due to the change in the core moiety.



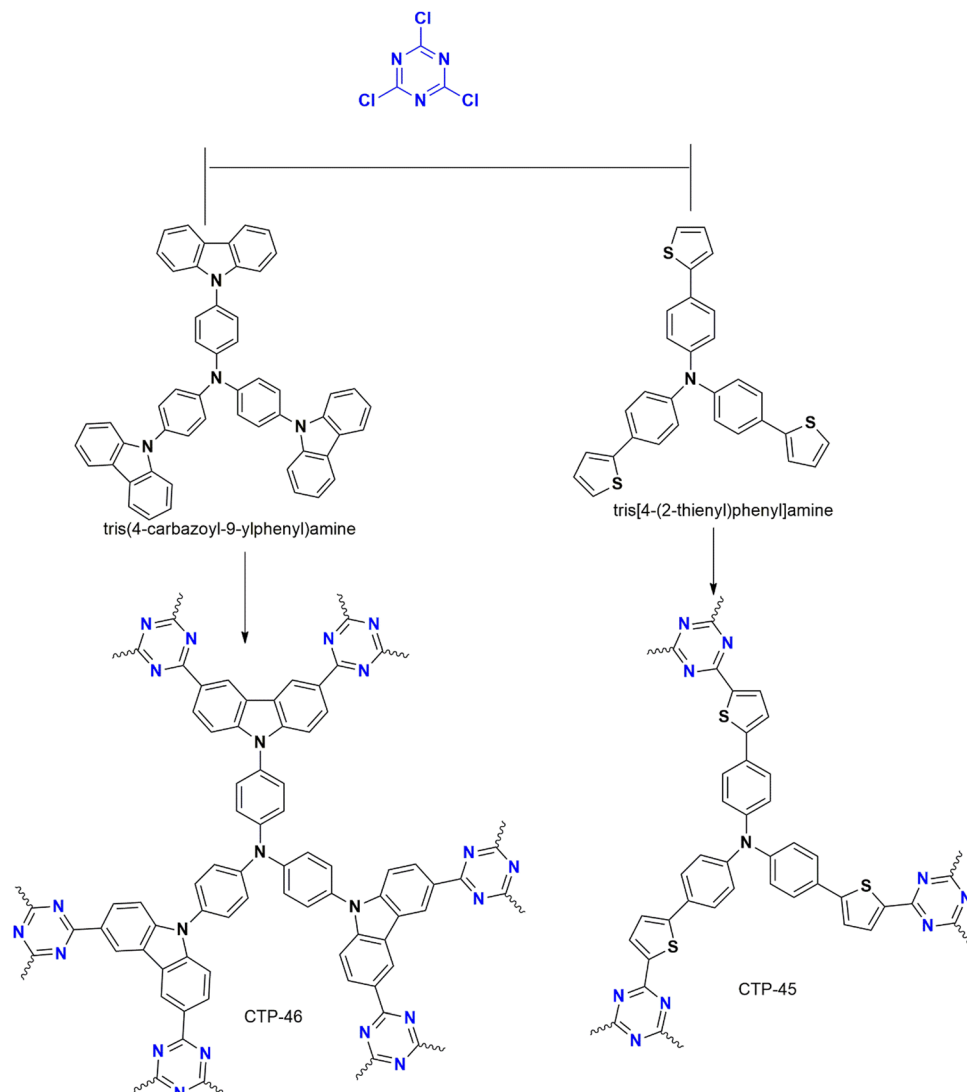


Fig. 52 Scheme for synthesis of CTP-45 and CTP-46.

#### 4.5. Energy storage devices

Inspired by the idea of utilizing organic molecules to modify the inorganic catalyst to prevent aggregation from accessing the binding pockets, Chen *et al.* designed a hybrid polymer, CTP-35 from bulky monomers (Fig. 41). They have chosen triazine derivative, cyanuric chloride, and sterically hindering phenyl-derived polymeric silsesquioxane (POSS-P) to avoid stacking the polymeric layers and generate heteroatom-rich networks.<sup>99</sup> Here, the phenyl rings can covalently bond with the cyanuric carbon by substituting for chlorine atoms. They have varied the molar ratios of both monomers to generate different polymers represented by CTP-35-*xy* (*x*:*y* being the ratio of monomers). All these monomers were carbonized to a high temperature. They have explored the application of this polymer in solid phase extraction as discussed above. The polymer was fabricated to utilize its ability as an electrode (anode) in lithium battery–future battery. Here, CTP-35-81, having enhanced pore characteristics regarding volume and binding sites, was chosen as the anode. The charging/discharging cycles of lithium ions in

the electrode were analyzed. The polymer showed remarkable stability, high affinity for electrons, and conductivity. The lithium adsorption and storage can be attributed to the interaction of the metal ion with basic triazine N and triazine C, followed by phenyl rings in POSS-P. After 2000 cycles at the 2 A g<sup>-1</sup> current density, the polymer exhibited a release rate of 817 mA g<sup>-1</sup>.

#### 4.6. Fluorescent sensors

Many porous polymers have been explored as fluorescent sensors for nitroaromatic compounds and iodine.<sup>67,68</sup> In 2021, Geng *et al.* synthesized a triazine framework using cyanuric chloride as the core with thiophene and carbazole-derived triphenylamine as the linkers (CTP-45 and CTP-46) as an efficient sensor (Fig. 52) with fluorescence behavior for detecting nitro aromatic compounds including picric acid and iodine.<sup>111</sup> In addition to this, it can also retain the captured iodine. These polymers existed in aggregate forms with amorphous nature. They possess remarkable surface area as CTP-45

with  $1235\text{ m}^2\text{ g}^{-1}$  (pores at 1.65 nm) and CTP-46 with  $2501\text{ m}^2\text{ g}^{-1}$  (pores at 1.8 nm). The conjugation enhanced by thiophene, carbazole, and triazine system improves the fluorescence ability, whereas the non-planar triphenyl amine prevents the quenching effect due to aggregation. Both CTPs exhibited strong fluorescence when dispersed in THF and dioxane, respectively. Both frameworks could quench the fluorescence by adding pollutants, picric acid (fast response of 20s), and iodine, better than reported sensors. In the case of radioactive iodine, sensing is mainly due to the interaction between the CTP and polyiodides formed by charge transfer. However, the sensing ability of the iodine solution (66.82% and 52.13%) is lower than the gaseous phase (2.58 and  $3.82\text{ g g}^{-1}$ , respectively) due to the blocking of pores by the solvents. CTP-45 proved to be a better sensor than CTP-46 and other thiophene-derived sensors.

#### 4.7. Health-care applications

The physico-chemical properties of triazine polymers make them useful in various applications, as discussed earlier. However, their biological implications are less explored, mainly driven by their biocompatibility. In this context, some of their applications in the field of healthcare are discussed.

**4.7.1. Drug release.** Inorganic compounds and coordinatively linked metal frameworks<sup>112,113</sup> are widely studied as drug carriers. The biocompatibility and nontoxicity of these materials matter a lot in their applications.<sup>114</sup> In 2011, Zhao and his co-workers synthesized a porous framework (CTP-11) from cyanuric chloride and piperazine by a cost-efficient moderate nucleophilic reaction (Fig. 17). The framework exhibited a structural regularity(partial crystalline) and morphological regularity (plate-like). They are thermally stable with reasonable surface area ( $182.7\text{ m}^2\text{ g}^{-1}$ ) and pores centered at 1.18 nm – the presence of flexible linkers (like piperazine) and kinetically regulated reaction-induced lower crystallinity. CTP-11 was utilized to uptake and release ibuprofen,<sup>115</sup> an anti-inflammatory drug. It was the first time an organic framework had been explored for such an application. Zero cellular toxicity was identified for CTP-11. 1 g of CTP-11 could absorb 0.35 g of ibuprofen. It exhibited an initial discharge (75% discharge rate) within 10 h. There was a discharge rate of 50% within five hours and complete discharge over 46 h. The discharge ability was better than MOFs<sup>113,116,117</sup> and comparable or superior to extensively researched inorganic mesoporous material MCM-41.<sup>118</sup> CTPs can be promoted as potential candidates for drug delivery because of ease of functionalization, stability, and porosity.

**4.7.2. Antibacterial agents.** To date, the antibacterial activity of porous polymers is attributed to oxidative destruction by singlet oxygen produced *in situ* by photon absorption of conjugated polymers *via* photosensitization. Porous polymers as effective antimicrobial agents have been rarely explored. In 2020, Rajagopal *et al.* designed a porous polymer CTP-15 (Fig. 21) from cyanuric chloride and methylated benzidine (*o*-tolidine) to investigate antibacterial activity.<sup>119</sup> The polymers are characterized as semi-crystalline, resembling graphitic carbons with irregular shapes and mesoporous in nature, with a

surface area of  $38\text{ m}^2\text{ g}^{-1}$ . Antibacterial action towards Gram-positive (*Staphylococcus aureus*) and Gram-negative (*Pseudomonas aeruginosa*) bacteria was evaluated by the optical density method (MIC value; minimum concentration to inhibit the bacterial growth in the culture medium) and the direct contact method (which calculates the colony forming unit) and compared with CTP-14 (cyanuric chloride crosslinked with phloroglucinol and *p*-phenylene diamine; Fig. 20). This comparison depicts the role of nitrogen functional groups towards antibacterial action. Both methods complement each other in showing that the two polymers exhibit the desired activity, preferring *P. aeruginosa* bacteria. CTP-15 outperformed CTP-14 with a low MIC value and zero colony formation. This remarkable ability of CTP-15 is due to a higher nitrogen ratio with triazine N and secondary amine N and a linear linker expanding the porosity. In CTP-14, oxygen linkage from phloroglucinol, in addition to nitrogen content, suppresses the inhibition rate. This widens the future scope of porous polymers in the biological arena.

## 5. Comparison with other porous materials

The realm of porous materials encompasses a variety of options, including activated carbon, zeolites, silica, metal organic frameworks (MOFs), and porous organic polymers (POPs). These materials are utilized across various applications due to their distinct surface properties, large surface area, and inherent porosity.

Activated carbon is characterized by a carbon-rich networked structure with a substantial surface area. On the other hand, zeolites are inorganic, hydrophilic porous materials, while MOFs are constructed from metal-centered organic polymers linked through weak coordination. While these materials exhibit efficient performance across different applications, they are susceptible to chemical instability and deactivation by moisture.<sup>14,120</sup> Additionally, the presence of metal linkers renders them non-biocompatible, and they often entail high-cost synthetic protocols. To overcome these limitations, attention has turned to these porous CTPs. These materials offer stability, rigidity, and distinctive porous characteristics while being free from metal, rendering them biocompatible, non-toxic, and requiring low synthetic strategies.

For pollutant adsorption, the previously mentioned porous materials have been utilized as adsorbents, albeit with limitations in adsorption capacity, stability, and reusability.<sup>121</sup> In contrast, CTPs have demonstrated efficiency as adsorbents due to their versatile interactions with adsorbates, facilitated by their functionalization, an attribute lacking in other porous materials despite their high surface area.<sup>122</sup>

Over the years, organic catalysis relied on enzyme-mediated or metal-based catalysts, necessitating the use of toxic and expensive chemicals and solvents, often leading to poor efficiency in purification and separation of the catalyst.<sup>31</sup> Subsequently, zeolites,<sup>123</sup> activated carbon,<sup>124</sup> silica,<sup>125</sup> and graphene oxides<sup>126</sup> were employed. However, due to stability concerns with the aforementioned materials, CTPs have emerged as



an alternative catalyst, serving as a solid support for immobilizing nanoparticles and enhancing catalytic activity.

Zeolites exhibit high adsorption capacity for  $\text{CO}_2$ , determined by their charge density and pore size. Conversely, their hydrophilic nature diminishes adsorption in humid climates, necessitating high regeneration temperatures.<sup>127,128</sup> Similarly, MOFs, being chemically unstable, exhibit limited gas adsorption.<sup>129</sup> Silica and activated carbon also display low adsorption capacity.<sup>128</sup> Contrastingly, CTPs have found wide application in gas adsorption and its separation,<sup>2</sup> solidifying their position as an emerging alternative porous material for various applications.

## 6. Conclusions

Over the years, researchers worldwide have been developing and investigating different triazine-rich porous polymers for potential applications. These polymers are rich in heteroatoms, mainly nitrogen, and exhibit excellent surface properties such as large surface area, pore diameter (in nm scale), and stable  $\text{C}=\text{N}$  bonds. They exhibit a larger surface area than other reported porous materials. As a result, they show promise as materials for addressing current research challenges.

This review provides an overview of the synthesis of various polymers (CTPs) using cyanuric chloride as a linker and inspects its applications across different domains. Cyanuric chloride is a cost-effective linker commonly employed in constructing these polymers. Its high reactivity, planar structure, and symmetric  $C_3$  point group allow for easy substitution with nucleophiles such as amines, alcohols, or aromatic hydrocarbons, resulting in polymerization in either two or three dimensions, depending on the conditions. Despite its irritant properties and low toxicity, it is valued as a superior cross-linking agent owing to its stable N-rich triazine structure, broadening its potential applications.

In exploring cost-effective synthetic protocols for CTPs, it becomes apparent that the Friedel–Crafts reaction surpasses traditional substitution reactions in terms of its environmentally friendly approach to enhancing surface properties, especially surface area. Nonetheless, it is crucial to acknowledge the limited applicability of Friedel–Crafts reactions in synthesizing certain polymers due to scalability challenges. The solvent-mediated synthesis protocols necessitate prolonged heating at high temperatures and use costly, hazardous solvents and catalysts. As a result, the synthetic strategies employing greener approaches, such as solid-state or environmentally friendly solvent medium, hold significant importance. Recently, the interest in mechanochemical approaches involving ball milling for synthesis has steadily increased.

The solubility of the building blocks in the solvent is a major concern that needs to be addressed for the polymer to precipitate during the reaction. The poor or partial solubility of cyanuric chloride in commonly used solvents, such as dichloromethane and dimethylformamide, can affect the reaction, resulting in low yield. The yield of the reaction has a significant impact and must be scaled up.

Most of the CTPs from cyanuric chloride reported in the literature are semi-crystalline or amorphous in nature. This is due to the stable  $\text{C}=\text{N}$  bonds and irreversible polymerizations. It is important to explore the development of crystalline CTPs with improved surface properties in the future.

The exceptional features of these CTPs include a stable heterogeneous nitrogen-rich triazine structure (catalyst and electrode materials), porous surface properties (adsorption and gas separation), low density (useful for hydrogen storage), and semiconductive nature (optics and photocatalysis). Many CTPs are currently being effectively utilized in the applications mentioned above. The nitrogen atom in the triazine rings can incorporate metal atoms (dopants), increasing the availability of active sites for binding and making them efficient catalysts. The porous structure, with its large surface area, can trap pollutants or gas molecules (acting as an adsorbent). Polymers with conjugated structures and widely spaced linkers decrease the band gap, enhancing charge transfer and optical properties (important for photocatalysis). Carbonization at higher temperatures enhances porosity and exposes active sites for electrochemical applications, but it may also degrade the polymer.

Advancements have been made in optimizing efficiency for different applications. One such advancement is post-functional modifications. Despite reducing surface area and porosity, these modifications help the polymer become a better absorbent or catalyst by exposing the binding sites. The chemical and thermal stability endowed by the polymer improves reusability and renewability (adsorption and catalysis). Magnetic polymeric composites have recently been examined in adsorption, simplifying the separation and filtration process. However, these polymers are less explored for biological applications. The biocompatibility of these polymers has to be discussed along with cytotoxic studies. It's important to further investigate these modifications for efficient applications.

The computational designing of these polymers and their evaluation in different applications has been relatively under-researched. This makes it easier to synthesize appropriate polymers for the required applications.

In most applications, CTPs have been found to outperform existing materials with comparable or better results. They can be used as an alternative to expensive metals in catalysis or for the adsorption of pollutants, carbon dioxide, and more. In addition, they can serve as a superior electrode material in energy storage devices. Therefore, CTPs are an advanced material capable of addressing major environmental and energy issues, and they open possibilities for further exploration in all fields. Despite the significant progress in the field of CTPs and their promising applications, there is still room for improvement in the synthetic protocols and their potential applications.

## Data availability

The data used in this article are properly cited in the manuscript. Also, where necessary, required permission is taken



form the concerned and presented in the manuscript. If required, the corresponding author can provide the data.

## Conflicts of interest

There are no conflicts to declare.

## References

- 1 M. Gomez, J. L. Gomez, M. D. Murcia, H. Peterson and N. Christofi, A New Kinetic Model for 4-Chlorophenol Adsorption on Expanded Clay, *Chem. Prod. Process Model.*, 2009, **4**(5), 1–6.
- 2 S.-P. Lee, N. Mellon, A. M. Shariff and J.-M. Leveque, Aromatic Polyamines Covalent Triazine Polymer as Sorbent for CO<sub>2</sub>Adsorption, *IOP Conf. Ser.: Mater. Sci. Eng.*, 2017, 226.
- 3 S. Jiao, L. Deng, X. Zhang, Y. Zhang, K. Liu and S. Li, *et al.*, Evaluation of an Ionic Porous Organic Polymer for Water Remediation, *ACS Appl. Mater. Interfaces*, 2021, **13**(33), 39404–39413.
- 4 A. Mukhtar, N. B. Mellon, M. A. Bustam, S. Saqib, S.-P. Lee and F. A. A. Kareem, *et al.*, Impact of amine functionality on the selective CO<sub>2</sub>/CH<sub>4</sub> adsorption behavior of porous covalent triazine adsorbent, *J. Nat. Gas Sci. Eng.*, 2020, 83.
- 5 N. S. Tadayoni, M. Dinari and A. Torbatian, Novel flower-like magnetic core-shell covalent triazine polymer as a beneficial Direct Scarlet 4BS adsorbent and comprehensive study of the kinetics and isotherm adsorption, *J. Environ. Chem. Eng.*, 2023, **11**(5), 1–15.
- 6 I. Thomas-Hillman, A. Laybourn, C. Dodds and S. W. Kingman, Realising the environmental benefits of metal–organic frameworks: recent advances in microwave synthesis, *J. Mater. Chem. A*, 2018, **6**(25), 11564–11581.
- 7 Y. Fan, B. Wang, S. Yuan, X. Wu, J. Chen and L. Wang, Adsorptive removal of chloramphenicol from wastewater by NaOH modified bamboo charcoal, *Bioresour. Technol.*, 2010, **101**(19), 7661–7664.
- 8 C. Moreno-Castilla, J. Rivera-Utrilla, M. V. López-Ramón and F. Carrasco-Marín, Adsorption of some substituted phenols on activated carbons from a bituminous coal, *Carbon*, 1995, **33**(6), 845–851.
- 9 Z. Li, J. Guo, Y. Wan, Y. Qin and M. Zhao, Combining metal–organic frameworks (MOFs) and covalent–organic frameworks (COFs): Emerging opportunities for new materials and applications, *Nano Res.*, 2021, **15**(4), 3514.
- 10 Z. Wang, Y. Zhang, G. Chang, J. Li, X. Yang and S. Zhang, *et al.*, Triazine-based covalent organic polymer: A promising coating for solid-phase microextraction, *J. Sep. Sci.*, 2021, **44**(19), 3608–3617.
- 11 Q. Sun, B. Aguilera, Y. Song and S. Ma, Tailored Porous Organic Polymers for Task-Specific Water Purification, *Acc. Chem. Res.*, 2020, **53**(4), 812–821.
- 12 H. R. Abuzeid, A. F. M. El-Mahdy and S.-W. Kuo, Covalent organic frameworks: Design principles, synthetic strategies, and diverse applications, *Giant*, 2021, 6.
- 13 V. Sadhasivam, M. Harikrishnan, G. Elamathi, R. Balasaravanan, S. Murugesan and A. Siva, Copper nanoparticles supported on highly nitrogen-rich covalent organic polymers as heterogeneous catalysts for the ipso-hydroxylation of phenyl boronic acid to phenol, *New J. Chem.*, 2020, **44**(16), 6222–6231.
- 14 Prakash K. Subodh and K. Chaudhary, Masram DT. A new triazine-cored covalent organic polymer for catalytic applications, *Appl. Catal., A*, 2020, 593.
- 15 M. Chaudhary and P. Mohanty, Nitrogen enriched polytriazine as a metal-free heterogeneous catalyst for the Knoevenagel reaction under mild conditions, *New J. Chem.*, 2018, **42**(15), 12924–12928.
- 16 D. Yadav and S. K. Awasthi, A Pd confined hierarchically conjugated covalent organic polymer for hydrogenation of nitroaromatics: catalysis, kinetics, thermodynamics and mechanism, *Green Chem.*, 2020, **22**(13), 4295–4303.
- 17 W. Dai, Q. Li, J. Long, P. Mao, Y. Xu and L. Yang, *et al.*, Hierarchically mesoporous imidazole-functionalized covalent triazine framework: An efficient metal- and halogen-free heterogeneous catalyst towards the cycloaddition of CO<sub>2</sub>with epoxides, *J. CO<sub>2</sub> Util.*, 2022, 62.
- 18 Y. Q. Dou, X. Yang, Q. Wang, Z. D. Yang, A. J. Wang and L. Zhao, *et al.*, Efficient hydrogen generation of a cobalt porphyrin-bridged covalent triazine polymer, *J. Colloid Interface Sci.*, 2023, **644**, 256–263.
- 19 S. Ren, R. Dawson, A. Laybourn, J.-X. Jiang, Y. Khimyak and D. J. Adams, *et al.*, Functional conjugated microporous polymers: from 1,3,5-benzene to 1,3,5-triazine, *Polym. Chem.*, 2012, **3**(4), 928–934.
- 20 P. Kuhn, M. Antonietti and A. Thomas, Porous, Covalent Triazine-Based Frameworks Prepared by Ionothermal Synthesis, *Angew. Chem., Int. Ed.*, 2008, **47**(18), 3450–3453.
- 21 S. Ren, M. J. Bojdys, R. Dawson, A. Laybourn, Y. Z. Khimyak and D. J. Adams, *et al.*, Porous, fluorescent, covalent triazine-based frameworks via room-temperature and microwave-assisted synthesis, *Adv. Mater.*, 2012, **24**(17), 2357–2361.
- 22 Z. Babaei, A. N. Chermahini, M. Dinari, M. Saraji and A. Shahvar, A sulfonated triazine-based covalent organic polymer supported on a mesoporous material: a new and robust material for the production of 5-hydroxymethylfurfural, *Sustainable Energy Fuels*, 2019, **3**(4), 1024–1032.
- 23 L. Liao, M. Li, Y. Yin, J. Chen, Q. Zhong and R. Du, *et al.*, Advances in the Synthesis of Covalent Triazine Frameworks, *ACS Omega*, 2023, **8**(5), 4527–4542.
- 24 A. Sethiya, D. K. Jangid, J. Pradhan and S. Agarwal, Role of cyanuric chloride in organic synthesis: A concise overview, *J. Heterocycl. Chem.*, 2023, **60**(9), 1495–1516.
- 25 B. Barton, S. Gouws, M. C. Schaefer and B. Zeelie, Evaluation and Optimisation of the Reagent Addition Sequence during the Synthesis of Atrazine (6-Chloro-N<sub>2</sub>-ethyl-N<sub>4</sub>-isopropyl-1,3,5-triazine-2,4-diamine) Using Reaction Calorimetry, *Org. Process Res. Dev.*, 2003, **7**(6), 1071–1076.
- 26 R. Tang, J. Wen, R. E. Stote and Y. Sun, Cyanuric Chloride-Based Reactive Dyes for Use in the Antimicrobial



Treatments of Polymeric Materials, *ACS Appl. Mater. Interfaces*, 2021, **13**(1), 1524–1534.

27 H. Q. Pham, T. T. Truong, D.-A. S. Nguyen and L.-T. T. Nguyen, Synthesis of a novel polymer via the coupling reaction of cyanuric chloride and a di-amine, *Vietnam J. Sci. Technol. Eng.*, 2020, **62**(2), 38–40.

28 D. Nardo, C. M. Akers, N. E. Cheung, C. M. Isom, J. T. Spaude and D. W. Pack, *et al.*, Cyanuric chloride as the basis for compositionally diverse lipids, *RSC Adv.*, 2021, **11**(40), 24752–24761.

29 S. Jain, J. Dwivedi, P. Jain and D. Kishore, Use of 2,4,6-trichloro-1,3,5-triazine (TCT) as organic catalyst in organic synthesis, *Synth. Commun.*, 2016, **46**(14), 1155–1174.

30 A. Chakraborty, S. Sarkar, R. Kyarikwal, P. Nag, S. R. Vennapusa and S. Mukhopadhyay, Piperazine-Linked Covalent Triazine Polymer as an Efficient Platform for the Removal of Toxic Mercury(II) Ions from Wastewater, *ACS Appl. Polym. Mater.*, 2022, **4**(11), 8118–8126.

31 D. Yadav and S. K. Awasthi, An unsymmetrical covalent organic polymer for catalytic amide synthesis, *Dalton Trans.*, 2020, **49**(1), 179–186.

32 Y. Xu, S. Jin, H. Xu, A. Nagai and D. Jiang, Conjugated microporous polymers: design, synthesis and application, *Chem. Soc. Rev.*, 2013, **42**(20), 8012–8031.

33 P. Zhang and S. Dai, Mechanochemical synthesis of porous organic materials, *J. Mater. Chem. A*, 2017, **5**(31), 16118–16127.

34 P. L. Cheung, S. K. Lee and C. P. Kubiak, Facile Solvent-Free Synthesis of Thin Iron Porphyrin COFs on Carbon Cloth Electrodes for CO<sub>2</sub> Reduction, *Chem. Mater.*, 2019, **31**(6), 1908–1919.

35 S. Verma, G. Kumar, A. Ansari and R. I. Kureshy, Khan N-uH. A nitrogen rich polymer as an organo-catalyst for cycloaddition of CO<sub>2</sub>to epoxides and its application for the synthesis of polyurethane, *Sustainable Energy Fuels*, 2017, **1**(7), 1620–1629.

36 T. Geng, S. Ye, Z. Zhu and W. Zhang, Triazine-based conjugated microporous polymers with *N,N,N',N'*-tetraphenyl-1,4-phenylenediamine, 1,3,5-tris(diphenylamino)-benzene and 1,3,5-tris[(3-methylphenyl)-phenylamino]benzene as the core for high iodine capture and fluorescence sensing of o-nitrophenol, *J. Mater. Chem. A*, 2018, **6**(6), 2808–2816.

37 S. Vargheese, M. Dinesh, K. V. Kavya, D. Pattappan, R. T. Rajendra Kumar and Y. Haldorai, Triazine-based 2D covalent organic framework-derived nitrogen-doped porous carbon for supercapacitor electrode, *Carbon Lett.*, 2021, **31**(5), 879–886.

38 T. Geng, M. Liu, C. Zhang, C. Hu and H. Y. Xia, The preparation of covalent triazine-based framework via Friedel-Crafts reaction of 2,4,6-trichloro-1,3,5-triazine with *N,N'*-diphenyl-*N,N'*-di(m-tolyl)benzidine for capturing and sensing to iodine, *Polym. Adv. Technol.*, 2020, **31**(6), 1388–1394.

39 X. Fu, Y. Zhang, S. Gu, Y. Zhu, G. Yu and C. Pan, *et al.*, Metal Microporous Aromatic Polymers with Improved Performance for Small Gas Storage, *Chem. – Eur. J.*, 2015, **21**(38), 13357–13363.

40 T. Geng, Z. Zhu, W. Zhang and Y. Wang, A nitrogen-rich fluorescent conjugated microporous polymer with triazine and triphenylamine units for high iodine capture and nitro aromatic compound detection, *J. Mater. Chem. A*, 2017, **5**(16), 7612–7617.

41 S. Xiong, X. Fu, L. Xiang, G. Yu, J. Guan and Z. Wang, *et al.*, Liquid acid-catalysed fabrication of nanoporous 1,3,5-triazine frameworks with efficient and selective CO<sub>2</sub> uptake, *Polym. Chem.*, 2014, **5**(10), 3424–3431.

42 P. Puthiaraj, S.-S. Kim and W.-S. Ahn, Covalent triazine polymers using a cyanuric chloride precursor via Friedel-Crafts reaction for CO<sub>2</sub> adsorption/separation, *Chem. Eng. J.*, 2016, **283**, 184–192.

43 S. Vargheese, M. Dinesh, K. V. Kavya, D. Pattappan, R. T. Rajendra Kumar and Y. Haldorai, Triazine-based 2D covalent organic framework-derived nitrogen-doped porous carbon for supercapacitor electrode, *Carbon Lett.*, 2020, **31**(5), 879–886.

44 S. Vargheese, R. T. R. Kumar and Y. Haldorai, Synthesis of triazine-based porous organic polymer: A new material for double layer capacitor, *Mater. Lett.*, 2019, **249**, 53–56.

45 X.-C. Fang, T.-M. Geng, F.-Q. Wang and W.-H. Xu, The synthesis of conjugated microporous polymers via Friedel-Crafts reaction of 2,4,6-trichloro-1,3,5-triazine with thieryl derivatives for fluorescence sensing to 2,4-dinitrophenol and capturing iodine, *J. Solid State Chem.*, 2022, 307.

46 E. Troschke, S. Grätz, T. Lübken and L. Borchardt, Mechanochemical Friedel-Crafts Alkylation—A Sustainable Pathway Towards Porous Organic Polymers, *Angew. Chem., Int. Ed.*, 2017, **56**(24), 6859–6863.

47 S. Pourebrahimi, M. Pirooz, A. De Visscher and G. H. Peslherbe, Highly efficient and reversible iodine capture utilizing amorphous conjugated covalent triazine-based porous polymers: Experimental and computational studies, *J. Environ. Chem. Eng.*, 2022, **10**(3), 107805.

48 H. Bildirir, Post-synthetic sulfonation of a diphenylanthracene based porous aromatic framework, *Org. Commun.*, 2022, 1–10.

49 Z. Li, Z. Liu, H. Li, M. Hasan, A. Suwansoontorn and G. Du, *et al.*, Sulfonated Triazine-Based Porous Organic Polymers for Excellent Proton Conductivity, *ACS Appl. Polym. Mater.*, 2020, **2**(8), 3267–3273.

50 R. Ghiai, S. Alavinia and R. Ghorbani-Vaghei, Chlorosulfonic acid coated on porous organic polymer as a bifunctional catalyst for the one-pot three-component synthesis of 1,8-naphthyridines, *RSC Adv.*, 2022, **12**(43), 27723–27735.

51 A. A. Raza, S. Ravi, S. S. Tajudeen and A. K. I. Sheriff, Trifunctional covalent triazine and carbonyl based polymer as a catalyst for one-pot multistep organic transformation, *React. Funct. Polym.*, 2021, **167**, 105011.

52 A. A. Raza, S. Ravi, S. S. Tajudeen and A. K. I. Sheriff, Sulfonated covalent triazine polymer loaded with Pd nanoparticles as a bifunctional catalyst for one pot hydrogenation esterification reaction, *J. Solid State Chem.*, 2021, **302**, 122417.

53 N. Taheri and M. Dinari, Development of sulfonic acid-functionalized covalent organic polymer towards efficient



adsorption of cationic dyes, *Appl. Surf. Sci. Adv.*, 2023, **18**, 100543.

54 E. Saputra, B. A. Prawiranegara, H. Sugesti, M. W. Nugraha and P. S. Utama, Covalent triazine framework: Water treatment application, *J. Water Process. Eng.*, 2022, **48**.

55 M. Liu, L. Guo, S. Jin and B. Tan, Covalent triazine frameworks: synthesis and applications, *J. Mater. Chem. A*, 2019, **7**(10), 5153–5172.

56 L. Shao, Y. Li, J. Huang and Y.-N. Liu, Synthesis of Triazine-Based Porous Organic Polymers Derived N-Enriched Porous Carbons for CO<sub>2</sub> Capture, *Ind. Eng. Chem. Res.*, 2018, **57**(8), 2856–2865.

57 H. Lundberg, F. Tinnis, N. Selander and H. Adolfsson, Catalytic amide formation from non-activated carboxylic acids and amines, *Chem. Soc. Rev.*, 2014, **43**(8), 2714–2742.

58 F. de Azambuja, J. Lenie and T. N. Parac-Vogt, Homogeneous Metal Catalysts with Inorganic Ligands: Probing Ligand Effects in Lewis Acid Catalyzed Direct Amide Bond Formation, *ACS Catal.*, 2021, **11**(1), 271–277.

59 C. Zou, M. Zhao and C. D. Wu, Synthesis of a porphyrinic polymer for highly efficient oxidation of arylalkanes in water, *Catal. Commun.*, 2015, **66**, 116–120.

60 P. Puthiaraj and K. Pitchumani, Palladium nanoparticles supported on triazine functionalised mesoporous covalent organic polymers as efficient catalysts for Mizoroki–Heck cross coupling reaction, *Green Chem.*, 2014, **16**(9), 4223–4233.

61 R. K. Yadav, A. Kumar, N. J. Park, K. J. Kong and J. O. Baeg, A highly efficient covalent organic framework film photocatalyst for selective solar fuel production from CO<sub>2</sub>, *J. Mater. Chem. A*, 2016, **4**(24), 9413–9418.

62 C. Zou, M. Zhao and C.-D. Wu, Synthesis of a porphyrinic polymer for highly efficient oxidation of arylalkanes in water, *Catal. Commun.*, 2015, **66**, 116–120.

63 W. Dai, Q. Li, J. Long, P. Mao, Y. Xu and L. Yang, *et al.*, Hierarchically mesoporous imidazole-functionalized covalent triazine framework: An efficient metal- and halogen-free heterogeneous catalyst towards the cycloaddition of CO<sub>2</sub> with epoxides, *J. CO<sub>2</sub> Util.*, 2022, **62**.

64 A. Liu, J. Zhang and X. Lv, Novel hydrazine-bridged covalent triazine polymer for CO<sub>2</sub> capture and catalytic conversion, *Chin. J. Catal.*, 2018, **39**(8), 1320–1328.

65 X. Li, C. Zhang, M. Luo, Q. Yao and Z.-H. Lu, Ultrafine Rh nanoparticles confined by nitrogen-rich covalent organic frameworks for methanolysis of ammonia borane, *Inorg. Chem. Front.*, 2020, **7**(5), 1298–1306.

66 D. Yadav, A. K. Dixit, S. Raghothama and S. K. Awasthi, Ni nanoparticle-confined covalent organic polymer directed diaryl-selenides synthesis, *Dalton Trans.*, 2020, **49**(35), 12266–12272.

67 A. Panalukudiyil Vijayan, A. Pallikkara, K. Ramakrishnan, R. S. Kumar and E. G. Jayasree, A Triazine Based Porous Organic Polymer as an Efficient Hydrogen-Bond Donor and Acceptor Cooperative Heterogeneous Catalyst for the Synthesis of 2-Substituted Benzimidazoles, *ChemistrySelect*, 2023, **8**(42), e202303092.

68 G. S. Lee, D. Kim and S. H. Hong, Pd-catalyzed formal Mizoroki–Heck coupling of unactivated alkyl chlorides, *Nat. Commun.*, 2021, **12**, 1.

69 I. Beletskaya, V. S. Tyurin, A. Y. Tsivadze, R. Guilard and C. Stern, Supramolecular Chemistry of Metalloporphyrins, *Chem. Rev.*, 2009, **109**(5), 1659–1713.

70 K. van Beurden, S. de Koning, D. Molendijk and J. van Schijndel, The Knoevenagel reaction: a review of the unfinished treasure map to forming carbon–carbon bonds, *Green Chem. Lett. Rev.*, 2020, **13**(4), 349–364.

71 E. V. Dalessandro, H. P. Collin, L. G. L. Guimarães, M. S. Valle and J. R. Pliego, Mechanism of the Piperidine-Catalyzed Knoevenagel Condensation Reaction in Methanol: The Role of Iminium and Enolate Ions, *J. Phys. Chem. B*, 2017, **121**(20), 5300–5307.

72 J. M. Humphrey and A. R. Chamberlin, Chemical Synthesis of Natural Product Peptides: Coupling Methods for the Incorporation of Noncoded Amino Acids into Peptides, *Chem. Rev.*, 1997, **97**(6), 2243–2266.

73 J. S. Carey, D. Laffan, C. Thomson and M. T. Williams, Analysis of the reactions used for the preparation of drug candidate molecules, *Org. Biomol. Chem.*, 2006, **4**(12), 2337–2347.

74 A. I. Alfano, H. Lange and M. Brindisi, Amide Bonds Meet Flow Chemistry: A Journey into Methodologies and Sustainable Evolution, *ChemSusChem*, 2022, **15**(6), e202102708.

75 V. Alagarsamy, K. Chitra, G. Saravanan, V. R. Solomon, M. T. Sulthana and B. Narendhar, An overview of quinazolines: Pharmacological significance and recent developments, *Eur. J. Med. Chem.*, 2018, **151**, 628–685.

76 J. Wu, Y.-F. Yang, X.-B. Huang, W.-X. Gao, Y.-B. Zhou and M.-C. Liu, *et al.*, Three-Component Reactions of Alkynone o-Methyloximes, Element Selenium, and Boronic Acids Leading to 4-Organoselenylisoxazoles, *ACS Omega*, 2020, **5**(36), 23358–23363.

77 S. Gopi and M. Kathiresan, 1,4-Phenylenediamine based covalent triazine framework as an electro catalyst, *Polymer*, 2017, **109**, 315–320.

78 V. Rajagopal, M. Ragunath, N. A. Khan, M. Kathiresan, V. Suryanarayanan and L. A. Jones, *et al.*, Gold nanoparticles decorated covalent organic polymer as a bimodal catalyst for total water splitting and nitro compound reduction. *Materials Today, Chemistry*, 2023, **27**, 101327.

79 S. Chen, Y. Zheng, B. Zhang, Y. Feng, J. Zhu and J. Xu, *et al.*, Cobalt, Nitrogen-Doped Porous Carbon Nanosheet-Assembled Flowers from Metal-Coordinated Covalent Organic Polymers for Efficient Oxygen Reduction, *ACS Appl. Mater. Interfaces*, 2018, **11**(1), 1384–1393.

80 V. Rajagopal, M. Kathiresan, P. Manivel, V. Suryanarayanan, D. Velayutham and K.-C. Ho, Porous organic polymer derived metal-free carbon composite as an electrocatalyst for CO<sub>2</sub> reduction and water splitting, *J. Taiwan Inst. Chem. Eng.*, 2020, **106**, 183–190.

81 V. Rajagopal, M. Manivannan, M. Kathiresan, V. Suryanarayanan and L. A. Jones, Metal/metal oxide-decorated covalent organic frameworks as electrocatalysts



for electrocarboxylation and water splitting, *Mater. Chem. Phys.*, 2022, **285**, 126104.

82 Y. Liu, W. Xu, W. Zhuge, Q. Huang, G. Xiang and J. Peng, Conductive aluminum phthalocyanine-based porous organic polymer as an efficient electrocatalyst for nifedipine detection, *Sens. Actuators, B*, 2024, **404**, 135191.

83 Z. Liang, H.-Y. Wang, H. Zheng, W. Zhang and R. Cao, Porphyrin-based frameworks for oxygen electrocatalysis and catalytic reduction of carbon dioxide, *Chem. Soc. Rev.*, 2021, **50**(4), 2540–2581.

84 S. N. Reddy, S. Nanda, D.-V. N. Vo, T. D. Nguyen, V.-H. Nguyen, B. Abdullah, *et al.*, in *Hydrogen: fuel of the near future, New Dimensions in Production and Utilization of Hydrogen*, 2020, pp. 1–20.

85 R. K. Yadav, A. Kumar, N.-J. Park, K.-J. Kong and J.-O. Baeg, A highly efficient covalent organic framework film photocatalyst for selective solar fuel production from CO<sub>2</sub>, *J. Mater. Chem. A*, 2016, **4**(24), 9413–9418.

86 K. Wu, P.-W. Cheng, X.-Y. Liu, J. Zheng, X.-W. Zhu and M. Xie, *et al.*, Polarization engineering in porous organic polymers for charge separation efficiency and its applications in photocatalytic aerobic oxidations, *Sci. China: Chem.*, 2024, **67**(3), 1000–1007.

87 P. Tang, B. Ji and G. Sun, Wearable super-adsorptive fibrous equipment in situ grafted with porous organic polymers for carcinogenic fumigant defense and detoxification, *J. Mater. Chem. A*, 2020, **8**(45), 24128–24136.

88 A. E. Kojo, W. Cho and C. Park, Mildly oxidized porous covalent triazine frameworks with rapid and high adsorption capability for aqueous organic micropollutants, *J. Ind. Eng. Chem.*, 2022, **116**, 250–256.

89 J. Wu, J. Liu, B. Wen, Y. Li, B. Zhou and Z. Wang, *et al.*, Nitrogen-rich covalent triazine frameworks for high-efficient removal of anion dyes and the synergistic adsorption of cationic dyes, *Chemosphere*, 2021, **272**, 129622.

90 Y.-C. Lu, J.-P. Yang, B.-T. Yang, C.-C. Chen and L.-L. Lai, Introduction of a spiro-linker in triazine-based polymers to enlarge void space and increase IPA adsorbing capacity to 164.7 mg g<sup>-1</sup> at 1000 ppm, *J. Taiwan Inst. Chem. Eng.*, 2022, **140**, 104531.

91 A. Sanjabi, S. Azizian, M. Torabi, M. A. Zolfigol and M. Yarie, On the applicability of triazine-based covalent organic polymer as adsorbent for dye removal from aqueous solution, *Microporous Mesoporous Mater.*, 2023, 348.

92 J. Yan, H. Sun, Q. Wang, L. Lu, B. Zhang and Z. Wang, *et al.*, Covalent triazine frameworks for the dynamic adsorption/separation of benzene/cyclohexane mixtures, *New J. Chem.*, 2022, **46**(16), 7580–7587.

93 Y. Xu, H. Yu, B. Shi, S. Gao, L. Zhang and X. Li, *et al.*, Room-Temperature Synthesis of Hollow Carbazole-Based Covalent Triazine Polymers with Multiactive Sites for Efficient Iodine Capture-Catalysis Cascade Application, *ACS Appl. Polym. Mater.*, 2020, **2**(8), 3704–3713.

94 F. Khosravi Esmaeilkhani, M. Dinari and N. Mokhtari, Nitrogen-rich porous organic polymer as a promising adsorbent for iodine capture from organic solvents, *New J. Chem.*, 2024, **48**(5), 1943–1951.

95 D. Wang, R. Zhang, Q. Zhang, H. Zhou and J. Sun, Reversible capture and release of I<sub>2</sub> with dechlorinated porous organic polymer, *Polymer*, 2024, **290**, 126592.

96 B. Lellis, C. Z. Fávaro-Polonio, J. A. Pamphile and J. C. Polonio, Effects of textile dyes on health and the environment and bioremediation potential of living organisms, *Biotechnol. Res. Innov.*, 2019, **3**(2), 275–290.

97 X. Chen, X. Wu, T. Luan, R. Jiang and G. Ouyang, Sample preparation and instrumental methods for illicit drugs in environmental and biological samples: A review, *J. Chromatogr. A*, 2021, 1640.

98 S. Dowlatshah, M. Saraji, M. Dinari and R. Soltani, A novel nanocomposite based on covalent organic polymer and nanocellulose for thin-film microextraction of imipramine from biological samples, *J. Sep. Sci.*, 2021, **44**(15), 2972–2981.

99 L. Chen, S. Chen, R. Fu and J. Zheng, Releasing the π-conjugated stack in triazine-derived porous materials for highly accessible active sites, *Chem. Eng. J.*, 2022, **443**, 136345.

100 X. Weng, S. Liu, J. Huang, Y. Lv, Y. Liu and X. Li, *et al.*, Efficient dispersive solid phase extraction of trace nitrophenol pollutants in water with triazine porous organic polymer modified nanofiber membrane, *J. Chromatogr. A*, 2024, **1717**, 464707.

101 Z. Wang, M. He, B. Chen and B. Hu, Triazine covalent organic polymer coated stir bar sorptive extraction coupled with high performance liquid chromatography for the analysis of trace phthalate esters in mineral water and liquor samples, *J. Chromatogr. A*, 2021, 1660.

102 G. Chang, Y. Zhao, B. Zhao, X. Yang, S. Zhang and C. Wang, *et al.*, A hydrophilic-lipophilic triazine based hyper-crosslinked polymer for efficient enrichment of nitrobenzene compounds, *Anal. Chim. Acta*, 2023, **1238**, 340638.

103 L. Meng, X. Zou, S. Guo, H. Ma, Y. Zhao and G. Zhu, Self-Supported Fibrous Porous Aromatic Membranes for Efficient CO<sub>2</sub>/N<sub>2</sub> Separations, *ACS Appl. Mater. Interfaces*, 2015, **7**(28), 15561–15569.

104 I. Sunarno, S.-P. Lee, N. Mellon, A. M. Shariff, J.-M. Leveque and A. Pulung Sasmito, *et al.*, Adsorption of CO<sub>2</sub> and Methane on Covalent Organic Polymer, *E3S Web Conf.*, 2018, 43.

105 C. Duan, Z. Du, W. Zou, H. Li and C. Zhang, Construction of Nitrogen-Containing Hierarchical Porous Polymers and Its Application on Carbon Dioxide Capturing, *Ind. Eng. Chem. Res.*, 2018, **57**(15), 5291–5300.

106 A. E. Sadak, A comparative gas sorption study of carbazole-derived microporous hyper-crosslinked polymers, *Microporous Mesoporous Mater.*, 2021, **311**, 110727.

107 E. Cucu, E. Dalkılıç, R. Altundas and A. E. Sadak, Gas sorption and selectivity study of N,N,N',N'-tetraphenyl-1,4-phenylenediamine based microporous hyper-crosslinked polymers, *Microporous Mesoporous Mater.*, 2022, 330.



108 S.-P. Lee, N. Mellon, A. M. Shariff and J.-M. Leveque, Effect of Diaminopropane on Formation of Triazine-based Covalent Organic Polymer for CO<sub>2</sub> Capture, *Procedia Eng.*, 2016, **148**, 184–188.

109 Y. Zhou, Z. Xiang, D. Cao and C.-J. Liu, Covalent organic polymer supported palladium catalysts for CO oxidation, *Chem. Commun.*, 2013, **49**(50), 5633–5635.

110 X. Du, Y. Cheng, Z. Liu, Z. Hou, T. Wu and R. Lei, *et al.*, Study on the adsorption of CH<sub>4</sub>, CO<sub>2</sub> and various CH<sub>4</sub>/CO<sub>2</sub> mixture gases on shale, *Alexandria Eng. J.*, 2020, **59**(6), 5165–5178.

111 T.-M. Geng, X.-C. Fang, F.-Q. Wang and F. Zhu, The Synthesis of Covalent Triazine-Based Frameworks via Friedel–Crafts Reactions of Cyanuric Chloride with Thiényl and Carbazolyl Derivatives for Fluorescence Sensing to Picric Acid, Iodine and Capturing Iodine, *Macromol. Mater. Eng.*, 2021, **306**(11), 2100461.1–2100461.10.

112 Y. Sun, L. Zheng, Y. Yang, X. Qian, T. Fu and X. Li, *et al.*, Metal–Organic Framework Nanocarriers for Drug Delivery in Biomedical Applications, *Nano-Micro Lett.*, 2020, **12**(1), 1–29.

113 P. Horcajada, C. Serre, M. Vallet-Regí, M. Sebban, F. Taulelle and G. Férey, Metal-organic frameworks as efficient materials for drug delivery, *Angew. Chem., Int. Ed.*, 2006, **45**(36), 5974–5978.

114 D. Maliszewski and D. Drozdowska, Recent Advances in the Biological Activity of s-Triazine Core Compounds, *Pharmaceuticals*, 2022, **15**(2), 1–19.

115 H. Zhao, Z. Jin, H. Su, X. Jing, F. Sun and G. Zhu, Targeted synthesis of a 2D ordered porous organic framework for drug release, *Chem. Commun.*, 2011, **47**(22), 6389–6391.

116 P. Horcajada, C. Serre, G. Maurin, N. A. Ramsahye, F. Balas and M. Vallet-Regí, *et al.*, Flexible porous metal-organic frameworks for a controlled drug delivery, *J. Am. Chem. Soc.*, 2008, **130**(21), 6774–6780.

117 A. A. El-Binary, E. A. Toson, K. R. Shoueir, H. A. Aljohani and M. M. Abo-Ser, Metal-organic frameworks as efficient materials for drug delivery: Synthesis, characterization, antioxidant, anticancer, antibacterial and molecular docking investigation, *Appl. Organomet. Chem.*, 2020, **34**, 11.

118 M. Vallet-Regí, A. Rámila, R. P. del Real and J. Pérez-Pariente, A New Property of MCM-41: Drug Delivery System, *Chem. Mater.*, 2000, **13**(2), 308–311.

119 V. Rajagopal, N. Jothi Narayanan, M. Kathiresan, D. K. Pattanayak and V. Suryanarayanan, Triazine inter-linked covalent organic polymer as an efficient antibacterial agent, *Materials Today, Chemistry*, 2021, **19**.

120 F. Wang, L. Liao, X. Liu, J. Zhang and F. Wu, Porphyrin-based porous organic frameworks as efficient peroxidase mimics for selective detection of hydrogen peroxide and glucose, *Inorg. Chem. Commun.*, 2023, 155.

121 V. Parimelazhagan, P. Yashwath, D. Arukkani Pushparajan and J. Carpenter, Rapid Removal of Toxic Remazol Brilliant Blue-R Dye from Aqueous Solutions Using Juglans nigra Shell Biomass Activated Carbon as Potential Adsorbent: Optimization, Isotherm, Kinetic, and Thermodynamic Investigation, *Int. J. Mol. Sci.*, 2022, **23**(20), 12484.

122 N. A. Medellín-Castillo, L. A. González-Fernández, R. Ocampo-Pérez, R. Leyva-Ramos, G. Luiz-Dotto and R. Flores-Ramírez, *et al.*, Efficient removal of triclosan from water through activated carbon adsorption and photodegradation processes, *Environ. Res.*, 2024, **246**, 118162.

123 Y. Li and J. Yu, Emerging applications of zeolites in catalysis, separation and host–guest assembly, *Nat. Rev. Mater.*, 2021, **6**(12), 1156–1174.

124 D. Duan, D. Chen, L. Huang, Y. Zhang, Y. Zhang and Q. Wang, *et al.*, Activated carbon from lignocellulosic biomass as catalyst: A review of the applications in fast pyrolysis process, *J. Anal. Appl. Pyrolysis*, 2021, **158**, 105246.

125 B. Singh, J. Na, M. Konarova, T. Wakihara, Y. Yamauchi and C. Salomon, *et al.*, Functional Mesoporous Silica Nanomaterials for Catalysis and Environmental Applications, *Bull. Chem. Soc. Jpn.*, 2020, **93**(12), 1459–1496.

126 N. M. Julkapli and S. Bagheri, Graphene supported heterogeneous catalysts: An overview, *Int. J. Hydrogen Energy*, 2015, **40**(2), 948–979.

127 D. G. Boer, J. Langerak and P. P. Pescarmona, Zeolites as Selective Adsorbents for CO<sub>2</sub> Separation. ACS Applied Energy, *Materials*, 2023, **6**(5), 2634–2656.

128 H. Jedli, M. Almonnef, R. Rabhi, M. Mbarek, J. Abdessalem and K. Slimi, Activated Carbon as an Adsorbent for CO<sub>2</sub> Capture: Adsorption, Kinetics, and RSM Modeling, *ACS Omega*, 2024, **9**(2), 2080–2087.

129 C.-H. Yu, C.-H. Huang and C.-S. Tan, A Review of CO<sub>2</sub> Capture by Absorption and Adsorption, *Aerosol Air Qual. Res.*, 2012, **12**(5), 745–769.

